Ann. Rev. Fluid Mech. 1983. 15:461–512

FLOW IN CURVED PIPES

S. A. Berger and L. Talbot

Department of Mechanical Engineering, University of California, Berkeley, California 94720

L.-S. Yao

Department of Mechanical and Aerospace Engineering, Arizona State University, Tempe, Arizona 85281

1. INTRODUCTION

Although the systematic theoretical and experimental exploration of flow in curved conduits is of fairly recent origin, it has long been appreciated that the flow is considerably more complex than that in straight conduits. The earliest observation of this was in fact for open channel flow, where the effects of curvature are most evident and striking (Thomson 1876, 1877). In this century, Grindley & Gibson (1908) noticed the curvature effect on the flow through a coiled pipe in experiments on the viscosity of air. Williams et al. (1902) observed that the location of the maximum axial velocity is shifted toward the outer wall of a curved pipe. Later, Eustice (1910, 1911) demonstrated the existence of a secondary flow by injecting ink into water flowing through a coiled pipe.

There are a whole host of areas where such flows are of practical importance and where questions are raised regarding them. For example, since curved sections invariably arise in all piping systems, it is important to know the pressure drop in the developing and fully developed parts of the flow if one is to predict the pumping power needed to overcome curvature-induced pressure losses. Because the secondary motions can be expected to enhance heat exchange between the fluid and its surroundings, knowledge of the magnitude of this effect is important in designing

0066-4189/83/0115-0461$02.00

heat exchangers. Blood flow in the human arterial system has been of particular interest to fluid mechanicians in recent years (Pedley 1980). The largest vessel in this system, the aorta, is highly curved. Of particular interest concerning the flow in this vessel is the entry length—the distance required for the flow to become fully developed—and the location of sites of maximum and minimum wall shear stress. The entry length is relevant to the flow in other curved blood vessels, since there is some question whether there is sufficient distance between bifurcations for the flow in arteries to become fully developed; the secondary motions in curved flows would be expected to be important in this context. The sites of extrema in the wall shear are important in the aorta and other large curved arteries because these may be the sites of cholesterol buildup on vessel walls, and thus may play a major role in atherogenesis.

In this article we review as comprehensively as space permits what is known about the flow in curved tubes and pipes. In particular, we discuss developing and fully developed flows, both steady and unsteady, in rigid infinitely coiled pipes; the flow in finite bends; thermal effects; and more briefly multiphase flow, the flow of non-Newtonian fluids, and the effect of flexible walls. Laminar incompressible flows will be our primary concern. We do not consider curved open-channel flows, since they differ enough in analysis and application to receive separate attention. Our main emphasis will be on tubes or pipes with circular cross sections. Finally, while we make reference to experimental results throughout, we have thought it wise to devote a separate section to them, with emphasis on the most recent studies and experimental techniques.

Secondary flows appear whenever fluid flows in curved pipes or channels. Although such secondary motions can arise in a perfect inviscid fluid as a result of a nonuniform distribution of velocity at the entrance to the bend (Squire & Winter 1949, Hawthorne 1951), throughout this review we shall consider real viscous fluids for which the secondary flow can be attributed principally to the effect of the centrifugal pressure gradient in the main flow acting on the relatively stagnant fluid in the wall boundary layer.

We begin with the steady, laminar, incompressible flow in a rigid circular pipe of uniform curvature.

2. STEADY, LAMINAR FLOW IN A RIGID PIPE

Consider a circular pipe with cross-sectional radius a coiled in a circle of radius R. We introduce the toroidal coordinate system (r', α, θ) shown in Figure 1, where r' denotes the distance from the center of the (circular)

cross section of the pipe, α the angle between the radius vector and the plane of symmetry, and θ the angular distance of the cross section from the entry of the pipe. The corresponding velocity components are (u', v', w'). The following nondimensional variables are defined

$$r = \frac{r'}{a}, \qquad s = \frac{R\theta}{a}, \qquad t = \frac{\bar{W}_0 t'}{a}$$

$$\mathbf{q} = \frac{\mathbf{q}'}{\bar{W}_0}, \qquad p = \frac{p'}{\rho \bar{W}_0^2}, \tag{1}$$

(primes denote dimensional quantities, unprimed quantities are dimensionless) where t is the time, $\mathbf{q} = (u, v, w)$, p is the pressure, ρ the density, and $\bar{W}_0$ the mean axial velocity in the pipe. For convenience we begin by writing down the full governing equations for viscous flow in such a curved pipe, without yet imposing the restriction that the flow is steady; these are

$$u_r + \frac{u}{r}\frac{1 + 2\delta r\cos\alpha}{1 + \delta r\cos\alpha} + \frac{v_\alpha}{r} - \frac{\delta v \sin\alpha}{1 + \delta r\cos\alpha} + \frac{w_s}{1 + \delta r\cos\alpha} = 0, \tag{2a}$$

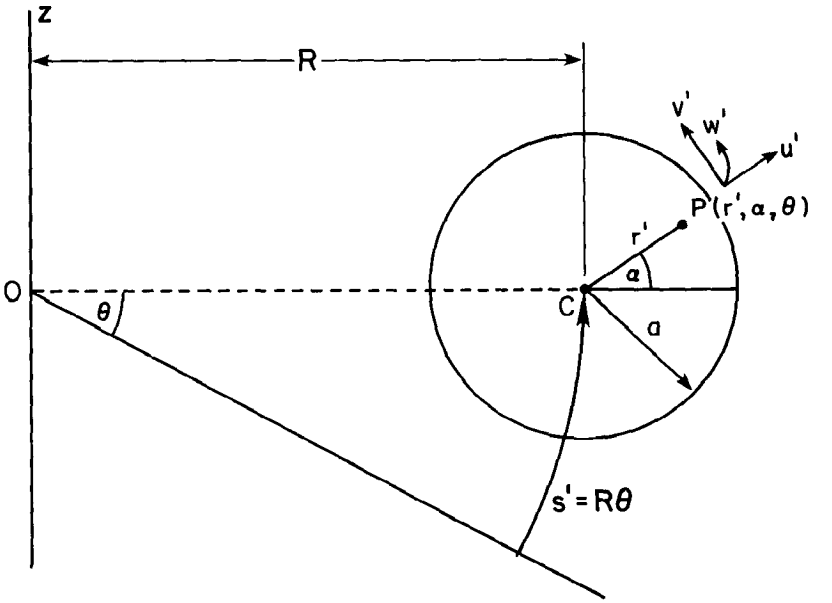

Figure 1 Toroidal coordinate system.

$$u_t + uu_r + \frac{vu_\alpha}{r} + \frac{wu_s}{1+\delta r\cos\alpha} - \frac{v^2}{r} - \frac{\delta w^2\cos\alpha}{1+\delta r\cos\alpha}$$

$$= -p_r - \frac{1}{\mathrm{Re}}\left[\left(\frac{1}{r}\frac{\partial}{\partial\alpha} - \frac{\delta\sin\alpha}{1+\delta r\cos\alpha}\right)\left(v_r + \frac{v}{r} - \frac{u_\alpha}{r}\right)\right. \tag{2b}$$

$$\left. - \frac{u_{ss}}{(1+\delta r\cos\alpha)^2} + \frac{1}{1+\delta r\cos\alpha}\left(w_{rs} + \frac{\delta w_s\cos\alpha}{1+\delta r\cos\alpha}\right)\right],$$

$$v_t + uv_r + \frac{vv_\alpha}{r} + \frac{wv_s}{1+\delta r\cos\alpha} + \frac{uv}{r} + \frac{\delta w^2\sin\alpha}{1+\delta r\cos\alpha}$$

$$= -\frac{p_\alpha}{r} + \frac{1}{\mathrm{Re}}\left[\frac{v_{ss}}{(1+\delta r\cos\alpha)^2} - \frac{w_{s\alpha}}{r(1+\delta r\cos\alpha)} + \frac{\delta w_s\sin\alpha}{(1+\delta r\cos\alpha)^2}\right. \tag{2c}$$

$$\left. + \left(\frac{\partial}{\partial r} + \frac{\delta\cos\alpha}{1+\delta r\cos\alpha}\right)\left(v_r + \frac{v}{r} - \frac{u_\alpha}{r}\right)\right],$$

$$w_t + uw_r + \frac{\delta uw\cos\alpha}{1+\delta r\cos\alpha} + \frac{vw_\alpha}{r} - \frac{\delta vw\sin\alpha}{1+\delta r\cos\alpha} + \frac{ww_s}{1+\delta r\cos\alpha}$$

$$= -\frac{p_s}{1+\delta r\cos\alpha} + \frac{1}{\mathrm{Re}}\left[\left(\frac{\partial}{\partial r} + \frac{1}{r}\right)\left(w_r + \frac{\delta w\cos\alpha}{1+\delta r\cos\alpha}\right) + \frac{w_{\alpha\alpha}}{r^2}\right. \tag{2d}$$

$$\left. - \frac{1}{r}\frac{\partial}{\partial\alpha}\left(\frac{\delta w\sin\alpha}{1+\delta r\cos\alpha}\right) - \left(\frac{\partial}{\partial r} + \frac{1}{r}\right)\frac{u_s}{1+\delta r\cos\alpha} - \frac{1}{r}\frac{\partial}{\partial\alpha}\left(\frac{v_s}{1+\delta r\cos\alpha}\right)\right],$$

(subscripts denote derivatives) where

$$\delta = \frac{a}{R} \quad \text{and} \quad \mathrm{Re} = \frac{a\overline{W}_0}{\nu}. \tag{3}$$

Here (2a) is the continuity equation and (2b–d) the momentum equations in the r, α, and s directions, respectively. [The reason for underlining the terms in (2b,c) is explained below.]

Nearly all analyses of this problem use as entry conditions either (*a*) constant total pressure across the cross section at the entrance:

$$\left.\begin{aligned} u &= v = 0, \\ w &= \frac{w'}{\overline{W}_0} = \frac{1}{1+\delta r\cos\alpha} \end{aligned}\right\} \text{at } \theta = 0, \tag{4a}$$

or (b) constant injection velocity:

$$\left.\begin{aligned} u = v = 0, \\ w = \frac{w'}{\overline{W}_0} = 1 \end{aligned}\right\} \text{ at } \theta = 0. \tag{4b}$$

(Occasionally, particularly if a straight section precedes the curved pipe, a Poiseuille profile is used as the entry condition.)

The boundary conditions of no slip at the pipe wall are

$$u = v = w = 0 \qquad \text{at} \qquad r = \frac{r'}{a} = 1. \tag{5}$$

Equations (2), (4a) or (4b), and (5) constitute the full formulation of the problem.

For the remainder of Section 2 we consider only steady flow, so the time derivative terms on the left-hand sides of (2b–d) are set equal to zero.

2.1 *Fully Developed Flow*

2.1.1 LOOSELY COILED PIPE At this point nearly all analyses assume that the pipe has only slight curvature, i.e. $\delta = a/R \ll 1$. Before dropping the $O(\delta)$ terms in (2a–d) compared with $O(1)$ terms, it is necessary to rescale the velocities to make the centrifugal-force terms in (2b,c), the underlined terms, of the same order of magnitude as the viscous and inertial terms, since it is the centrifugal force that drives the secondary motion. The transformation that accomplishes this is

$$(u, v, w) \rightarrow (\delta^{1/2}\hat{u}, \delta^{1/2}\hat{v}, \hat{w}). \tag{6}$$

In what follows we shall omit the caret sign, it being understood that the velocities that appear are those on the right-hand side of (6). It is also convenient to rescale the axial distance as follows:

$$s = \frac{R\theta}{a} = \delta^{-1/2} z. \tag{7}$$

The rescaled forms of (2) are

$$\frac{\partial u}{\partial r} + \frac{u}{r}\left(\frac{1 + 2\delta r\cos\alpha}{1 + \delta r\cos\alpha}\right) + \frac{1}{r}\frac{\partial v}{\partial \alpha} - \frac{\delta v \sin\alpha}{1 + \delta r\cos\alpha} + \frac{1}{1 + \delta r\cos\alpha}\frac{\partial w}{\partial z} = 0, \tag{8a}$$

$$u\frac{\partial u}{\partial r}+\frac{v}{r}\frac{\partial u}{\partial \alpha}+\frac{w}{1+\delta r\cos\alpha}\frac{\partial u}{\partial z}-\frac{v^2}{r}-\frac{w^2\cos\alpha}{1+\delta r\cos\alpha}$$
$$=-\frac{1}{\delta}\frac{\partial p}{\partial r}-\frac{2}{\kappa}\left\{\left(\frac{1}{r}\frac{\partial}{\partial \alpha}-\frac{\delta\sin\alpha}{1+\delta r\cos\alpha}\right)\left(\frac{\partial v}{\partial r}+\frac{v}{r}-\frac{1}{r}\frac{\partial u}{\partial \alpha}\right)\right.$$
$$-\frac{\delta}{(1+\delta r\cos\alpha)^2}\frac{\partial^2 u}{\partial z^2}$$
$$\left.+\frac{1}{1+\delta r\cos\alpha}\left(\frac{\partial^2 w}{\partial r\,\partial z}+\frac{\delta\cos\alpha}{1+\delta r\cos\alpha}\frac{\partial w}{\partial z}\right)\right\}, \tag{8b}$$

$$u\frac{\partial v}{\partial r}+\frac{v}{r}\frac{\partial v}{\partial \alpha}+\frac{w}{1+\delta r\cos\alpha}\frac{\partial v}{\partial z}+\frac{uv}{r}+\frac{w^2\sin\alpha}{1+\delta r\cos\alpha}$$
$$=-\frac{1}{r\delta}\frac{\partial p}{\partial \alpha}+\frac{2}{\kappa}\left\{\frac{\delta}{(1+\delta r\cos\alpha)^2}\frac{\partial^2 v}{\partial z^2}-\frac{1}{1+\delta r\cos\alpha}\frac{1}{r}\frac{\partial^2 w}{\partial\alpha\,\partial z}\right.$$
$$+\frac{\delta\sin\alpha}{(1+\delta r\cos\alpha)^2}\frac{\partial w}{\partial z}$$
$$\left.+\left(\frac{\partial}{\partial r}+\frac{\delta\cos\alpha}{1+\delta r\cos\alpha}\right)\left(\frac{\partial v}{\partial r}+\frac{v}{r}-\frac{1}{r}\frac{\partial u}{\partial \alpha}\right)\right\}, \tag{8c}$$

$$u\frac{\partial w}{\partial r}+\frac{\delta uw\cos\alpha}{1+\delta r\cos\alpha}+\frac{v}{r}\frac{\partial w}{\partial \alpha}-\frac{\delta\sin\alpha}{1+\delta r\cos\alpha}uw+\frac{w}{1+\delta r\cos\alpha}\frac{\partial w}{\partial z}$$
$$=-\frac{1}{1+\delta r\cos\alpha}\frac{\partial p}{\partial z}+\frac{2}{\kappa}\left\{\left(\frac{\partial}{\partial r}+\frac{1}{r}\right)\left(\frac{\partial w}{\partial r}+\frac{\delta w\cos\alpha}{1+\delta r\cos\alpha}\right)+\frac{1}{r^2}\frac{\partial^2 w}{\partial\alpha^2}\right.$$
$$-\frac{1}{r}\frac{\partial}{\partial\alpha}\left(\frac{\delta w\sin\alpha}{1+\delta r\cos\alpha}\right)-\left(\frac{\partial}{\partial r}+\frac{1}{r}\right)$$
$$\left.\times\frac{\delta}{1+\delta r\cos\alpha}\frac{\partial u}{\partial z}-\frac{1}{r}\frac{\partial}{\partial\alpha}\left(\frac{\delta}{1+\delta r\cos\alpha}\frac{\partial v}{\partial z}\right)\right\}, \tag{8d}$$

where κ, the Dean number, is defined as

$$\kappa=2\delta^{1/2}\mathrm{Re}=\left(\frac{a}{R}\right)^{1/2}\frac{2a\overline{W}_0}{\nu}. \tag{9}$$

From these governing equations we see that two parameters, κ and δ, characterize the flow in curved pipes. The Dean number κ is equal to the ratio of the square root of the product of the inertia and centrifugal forces to the viscous force. Since the secondary flow is induced by centrifugal forces and their interaction primarily with viscous forces, κ is a measure of the magnitude of the secondary flow. We note that no secondary flow will be induced for an inviscid fluid. The parameter δ is a more detailed measure of the effect of geometry and the extent to which the centrifugal force varies on the cross section. Thus δ affects the balance of inertia, viscous, and centrifugal forces, and while its influence has been studied much less than that of κ, it can play a major role in curved-pipe flows. This is discussed in Section 2.1.2.

We note that (8b) and (8c) are of the form

$$O(1) = -\frac{1}{\delta}\frac{\partial p}{\partial r}, \qquad O(1) = -\frac{1}{r\delta}\frac{\partial p}{\partial \alpha}. \tag{10}$$

Thus when $\delta \ll 1$, we may write

$$p = p_0(z) + \delta p_1(r, \alpha, z) + \ldots, \tag{11}$$

i.e. the major contribution to the axial pressure gradient may be separated from the cross-sectional component.

We can now consider the loosely coiled pipe limit by setting $\delta = 0$ in (8). Using (11), this yields the following reduced equations:

$$\frac{\partial u}{\partial r} + \frac{u}{r} + \frac{1}{r}\frac{\partial v}{\partial \alpha} + \frac{\partial w}{\partial z} = 0, \tag{12a}$$

$$u\frac{\partial u}{\partial r} + \frac{v}{r}\frac{\partial u}{\partial \alpha} + w\frac{\partial u}{\partial z} - \frac{v^2}{r} - w^2\cos\alpha = \frac{-\partial p_1}{\partial r} - \frac{2}{\kappa}\left\{\frac{1}{r}\frac{\partial}{\partial \alpha}\left(\frac{\partial v}{\partial r} + \frac{v}{r} - \frac{1}{r}\frac{\partial u}{\partial \alpha}\right) + \frac{\partial^2 w}{\partial r\,\partial z}\right\}, \tag{12b}$$

$$u\frac{\partial v}{\partial r} + \frac{v}{r}\frac{\partial v}{\partial \alpha} + w\frac{\partial v}{\partial z} + \frac{uv}{r} + w^2\sin\alpha = -\frac{1}{r}\frac{\partial p_1}{\partial \alpha} + \frac{2}{\kappa}\left\{\frac{-\partial^2 w}{r\,\partial\alpha\,\partial z} + \frac{\partial}{\partial r}\left(\frac{\partial v}{\partial r} + \frac{v}{r} - \frac{1}{r}\frac{\partial u}{\partial \alpha}\right)\right\}, \tag{12c}$$

$$u\frac{\partial w}{\partial r} + \frac{v}{r}\frac{\partial w}{\partial \alpha} + w\frac{\partial w}{\partial z} = \frac{-\partial p_0}{\partial z} + \frac{2}{\kappa}\left\{\left(\frac{\partial}{\partial r} + \frac{1}{r}\right)\frac{\partial w}{\partial r} + \frac{1}{r^2}\frac{\partial^2 w}{\partial \alpha^2}\right\}. \tag{12d}$$

The only nondimensional parameter appearing in these equations is the Dean number κ, which plays the role of a "Reynolds number" of the

flow and leads to the so-called Dean-number similarity, first noted by Dean (1928). Note that this is not the case for curved-pipe flows in general, but only when $\delta \ll 1$.

The flow is fully developed when it no longer varies with axial position. The governing equations, obtained by setting all z-derivatives, except that of the pressure, equal to zero in (12a–d), are

$$\frac{\partial u}{\partial r} + \frac{u}{r} + \frac{1}{r}\frac{\partial v}{\partial \alpha} = 0, \tag{13a}$$

$$u\frac{\partial u}{\partial r} + \frac{v}{r}\frac{\partial u}{\partial \alpha} - \frac{v^2}{r} - w^2\cos\alpha = -\frac{\partial p_1}{\partial r} - \frac{2}{\kappa}\frac{1}{r}\frac{\partial}{\partial \alpha}\left(\frac{\partial v}{\partial r} + \frac{v}{r} - \frac{1}{r}\frac{\partial u}{\partial \alpha}\right), \tag{13b}$$

$$u\frac{\partial v}{\partial r} + \frac{v}{r}\frac{\partial v}{\partial \alpha} + \frac{uv}{r} + w^2\sin\alpha = -\frac{1}{r}\frac{\partial p_1}{\partial \alpha} + \frac{2}{\kappa}\frac{\partial}{\partial r}\left(\frac{\partial v}{\partial r} + \frac{v}{r} - \frac{1}{r}\frac{\partial u}{\partial \alpha}\right), \tag{13c}$$

$$u\frac{\partial w}{\partial r} + \frac{v}{r}\frac{\partial w}{\partial \alpha} = -\frac{\partial p_0}{\partial z} + \frac{2}{\kappa}\left\{\left(\frac{\partial}{\partial r} + \frac{1}{r}\right)\frac{\partial w}{\partial r} + \frac{1}{r^2}\frac{\partial^2 w}{\partial \alpha^2}\right\}. \tag{13d}$$

The velocity components are now functions of r and α only; it then follows from (13d) that $\partial p_0/\partial z$ is independent of z and hence we can write $p_0(z) = -Gz$, where G is a constant.

Equation (13a) can be satisfied automatically by introducing a stream function for the secondary flow, defined by

$$u = \frac{1}{r}\frac{\partial \psi}{\partial \alpha}, \qquad v = -\frac{\partial \psi}{\partial r}. \tag{14}$$

Substitution into (13d) yields

$$\nabla_1^2 w - \frac{\kappa}{2}\frac{\partial p_0}{\partial z} = \frac{\kappa}{2r}(\psi_\alpha w_r - \psi_r w_\alpha), \tag{15}$$

while cross-differentiation of (13b,c) and elimination of the pressure yields

$$\frac{2}{\kappa}\nabla_1^4\psi + \frac{1}{r}\left(\psi_r\frac{\partial}{\partial \alpha} - \psi_\alpha\frac{\partial}{\partial r}\right)\nabla_1^2\psi = -2w\left(\sin\alpha w_r + \frac{\cos\alpha}{r}w_\alpha\right), \tag{16}$$

where

$$\nabla_1^2 \equiv \frac{\partial^2}{\partial r^2} + \frac{1}{r}\frac{\partial}{\partial r} + \frac{1}{r^2}\frac{\partial^2}{\partial \alpha^2}. \tag{17}$$

The boundary conditions are

$$\psi = \psi_r = w = 0 \quad \text{at} \quad r = 1. \tag{18}$$

Equations (15) and (16) for w and ψ, together with boundary conditions (18), a formulation originally given by Dean (1928), completely determine the problem for fully developed flow for a loosely coiled pipe.

2.1.1.1 *Small Dean number* For small values of the Dean number, Dean (1927, 1928) solved the above problem by expanding the solution in a series in powers of the Dean number, i.e.

$$w = \sum_{n=0}^{\infty} \kappa^{2n} w_n(r, \alpha), \qquad \psi = \kappa \sum_{n=0}^{\infty} \kappa^{2n} \psi_n(r, \alpha). \tag{19}$$

The leading term for w, w_0, is Poiseuille flow in a straight tube; the leading term for ψ is $O(\kappa)$. This series expansion in κ is equivalent to perturbing the equivalent Poiseuille flow and calculating the influence of the inertia terms by successive approximation, and is thus only appropriate for slightly, or loosely, coiled pipes or tubes. Figure 2 shows, for a typical case, secondary streamlines in the pipe cross section and

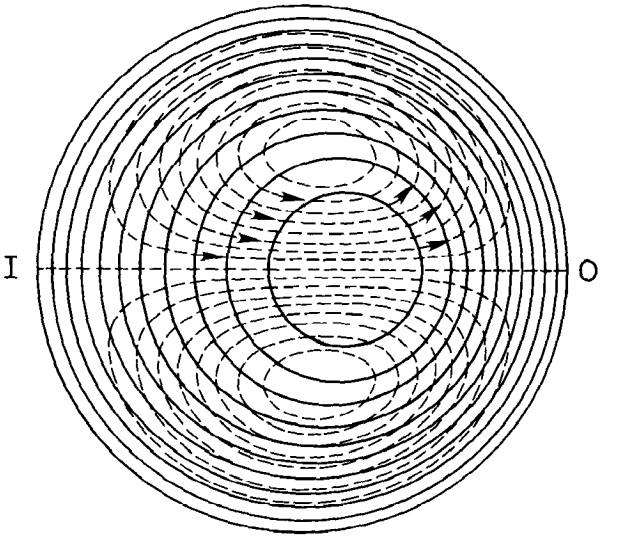

Figure 2 Secondary streamlines and axial-velocity contours at low Dean number. I denotes inner bend, O outer bend.

contours of constant axial velocity. The flow consists of a pair of counterrotating helical vortices, placed symmetrically with respect to the plane of symmetry. This secondary flow pattern arises because the centrifugally-induced pressure gradient, approximately uniform over the cross section, drives the slower-moving fluid near the wall inward, while the faster-moving fluid in the core is swept outward. The vortices are almost symmetrically placed with respect to $\alpha = \pm \pi/2$, with the stagnation points (or "centers") of the secondary vortices located on these lines at $r \approx 0.43$, while the position of maximum axial velocity moves outward to $r \approx 4.2 \times 10^{-4} K$, $\alpha = 0$.

The nondimensional volume flux in the pipe depends only on Dean number and is given by

$$\frac{Q}{\pi a^2 \overline{W}} = 1 - 0.0306\left(\frac{K}{576}\right)^2 + 0.0120\left(\frac{K}{576}\right)^4 + O\left[\left(\frac{K}{576}\right)^6\right], \qquad (20)$$

where $K = (2a/R)(W_{\max} a/\nu)^2$, $W_{\max}$ is the maximum velocity in a straight pipe of the same radius under the same axial pressure gradient, and $\overline{W}$ is the mean velocity in the same pipe (so $\overline{W} = \overline{W}_{\max}/2$). K is a variant of the Dean number, in the form first used by Dean (see Section 2.1.1.2 below). The first term on the right-hand side represents the Poiseuille straight-pipe value. Not surprisingly, we see that the effect of curvature is to reduce the flux. For example, when $K = 576$ the flux is reduced in consequence of the curvature by about 2%.

One outstanding feature of Dean's series solution is that the flow resistance is not affected by the first-order terms and is increased only by the second-order terms. This flow resistance is generally represented nondimensionally in terms of the friction factor, or ratio, λ (White 1929), the ratio of the resistance in the curved pipe (λ_c) to the resistance in a straight pipe (λ_s) carrying the same flux. Since this is equal to $(Q_c/Q_s)^{-1}$, where Q_c and Q_s are the fluxes in the curved and straight pipes, respectively, under the same pressure gradient, it follows from (20) that

$$\lambda = \frac{\lambda_c}{\lambda_s} = \left(\frac{Q_c}{Q_s}\right)^{-1} = 1 + 0.0306\left(\frac{K}{576}\right)^2 - 0.0110\left(\frac{K}{576}\right)^4 + \cdots \qquad (21)$$

Dean conjectured, from a consideration of the coefficients in (20), that his small-Dean-number series solution was valid for $K \lesssim 576$, a statement subsequently confirmed experimentally by White (1929) based on consideration of (21). Experiments (White 1929, Taylor 1929, Adler 1934) have also confirmed that the flow in a curved pipe or tube is much more stable than that in a straight pipe or tube, so whereas the critical Reynolds number for the latter is typically about 2000, in a curved tube, of even small curvature, it may be larger by a factor of two or more. For

example, Taylor found that for $a/R = 1/31.9$, the critical Reynolds number was about 5000.[1] This corresponds to $K \approx 1.6 \times 10^6$ and therefore approximately delineates the laminar regime over which calculated results would be of interest. Since the upper limit of validity of Dean's series solution ($K = 576$) obviously falls far short of covering the full laminar-flow range, we next consider solutions for larger values of Dean number. Before doing so, however, we digress for a moment to consider the question of the appropriate definition of Dean number.

2.1.1.2 *Definition of Dean number* In Equation (9), the Dean number κ was defined as

$$\kappa = 2\delta^{1/2}\mathrm{Re} = \left(\frac{a}{R}\right)^{1/2}\left(\frac{2a\overline{W}_0}{\nu}\right),$$

where $\overline{W}_0$ is the mean axial velocity in the pipe, while the original form of the Dean number was defined by Dean (1928) as

$$K = 2\left(\frac{a}{R}\right)\left(\frac{aW_0}{\nu}\right)^2 = \frac{2W_0^2a^3}{\nu^2R}, \tag{22}$$

where W_0 is defined only as a constant having the dimensions of a velocity. If we take $W_0 = \overline{W}_0$, then K and κ are related by $\kappa = (2K)^{1/2}$. For fully developed flow it follows from (2b–d) that the axial pressure gradient is constant, say $\partial p'/R\,\partial\theta = -G$ (G constant), in dimensional terms. We can then define a nondimensional constant, $C = Ga^2/\mu W_0$, and rewrite (22) as

$$K = \frac{2a^3}{\nu^2R}\left(\frac{Ga^2}{\mu C}\right)^2. \tag{23}$$

If, following Dean (1928), we specify W_0 as the maximum velocity ($W_{\max}$) in a straight pipe of the same radius and with the same pressure gradient, then $C = 4$ and (23) becomes

$$K = \frac{2a^3}{\nu^2R}\left(\frac{Ga^2}{4\mu}\right)^2 = 2\left(\frac{a}{R}\right)\left(\frac{Ga^3}{4\mu\nu}\right)^2 = \frac{G^2a^7}{8\mu^2\nu^2R} \tag{24}$$

whereas if we simply set $C = 1$, (23) becomes

$$K = \frac{2a^3}{\nu^2R}\left(\frac{Ga^2}{\mu}\right)^2. \tag{25}$$

[1]This effect of curvature seems never to have been explained. For a phenomenological conjecture based on recent ideas about coherent structures in turbulent flow, see Coles (1981). This can be contrasted with an earlier alternative explanation given by Lighthill (1970).

Since Dean's original work, most investigators have used not only all of the above variants of the Dean number, but to make matters even worse they have used $2a$ rather than a, or vice versa, in $\delta = a/R$ and the definition of Reynolds number, or they have used κ^2 or $K^{1/2}$ rather than κ or K. This obviously makes for considerable confusion in reading and interpreting the literature. [Van Dyke (1978) gives a useful compilation of the relationships between the various versions used in some of the most often cited papers.]

Versions of Dean number based on $\overline{W}_0$, the mean axial velocity, are natural for the experimentalist because this quantity, being readily measured, provides a more convenient characterization of the flow than the more difficult to measure pressure gradient. For fully developed flow it makes little difference whether one uses a form of Dean number based on $\overline{W}_0$ or any of the variants based on G, i.e. (23), since C = constant for such a flow. For these flows most theoretical and numerical investigators, beginning with McConalogue & Srivastava (1968), have used the square root of (25) and denoted this by D, i.e.

$$D = \left(\frac{2a^3}{\nu^2 R}\right)^{1/2} \frac{Ga^2}{\mu} = 4\left(\frac{2a}{R}\right)^{1/2} \frac{Ga^3}{4\mu\nu}, \tag{26}$$

which is related to the original Dean number, (24), by $D = 4K_{\text{Dean}}^{1/2}$. [Equations (20) and (21) can be rewritten in terms of D by replacing each of the factors $(K/576)^2$ by $(D/96)^4$.] The relationship between K or D and κ is more complicated, and depends on the flux ratio itself, according as

$$\frac{Q_c}{Q_s} = \frac{\kappa}{\left(\frac{1}{2}K\right)^{1/2}} = 2^{5/2}\frac{\kappa}{D} \tag{27}$$

(McConalogue 1970, Van Dyke 1978). Thus, while the relationship between K or D and κ is known a priori for values of Dean number small enough that $\overline{W}_0$ is related to G approximately as in Poiseuille flow, for larger values the relationship between these Dean numbers can only be determined a posteriori after the solution, and hence the flux ratio, is calculated.

For flows that are not fully developed the situation is even more complicated, for while $\overline{W}_0$ is a true constant for a pipe of given cross section and fixed flow conditions, the pressure gradient is, in general, a function both of axial location and position in the cross section. (For a loosely coiled pipe, to lowest order, see (11), it only depends on axial location.) Consequently C, the ratio of G to W_0, whatever the choice of W_0, is not a constant; moreover, this ratio is not known until the solution is obtained—the relationship between G and W_0 being one of the

principal objects of the investigation. Therefore, the forms of Dean number that follow from (23), e.g. (24) and (25), can be used for other than fully developed flows only if one specifies G in such a way that it is a constant. Since there is no a priori way of knowing how to do this so as to make the resulting Dean number properly characterize the flow, and in any case measurement of any such pressure gradient is likely to be difficult, it would appear that basing Dean number on the mean axial velocity, such as in (9), is preferable. To avoid the confusion described above we strongly suggest that future studies use the form (9) whether the flow is fully developed or not. This suggestion notwithstanding, the concerned reader should be wary in interpreting the literature—past, present, and future!

Finally, we note that in terms of the Dean number D, defined by (26), the upper limit of validity of Dean's series solution, corresponding to $K = 576$, is $D = 96$, while the upper limit of the laminar-flow regime is approximately $D = 5000$. We now discuss the work that has attempted to bridge this gap.

2.1.1.3 *Intermediate Dean number* Since, as we shall see in the next section, boundary-layer concepts are applicable to the flow at large Dean number, whereas for intermediate values one has to solve the full nonlinear equations (15) and (16) numerically, solutions in this range historically followed much of the well-known large-Dean-number work.

McConalogue & Srivastava (1968) obtained numerical solutions for the fully developed flow for the range $96 < D \lesssim 600$ by expanding in Fourier series (in α), then integrating the resulting ordinary differential equations (in r) numerically. Since then, many papers have reported finite-difference solutions, e.g. Truesdell & Adler (1970), Akiyama & Cheng (1971), Greenspan (1973), Austin & Seader (1973), Patankar et al. (1974), Collins & Dennis (1975), Zapryanov & Christov (1977), Dennis & Ng (1980, 1982), and Dennis (1980). Among these the most extensive, and certainly among the most reliable, are those of Collins & Dennis (1975), who solved (15) and (16) for the full laminar range $D = 96$–5000. Figure 3 shows the secondary streamlines and contours of constant axial velocity for $D = 96$ and 606 from the solutions of McConalogue & Srivastava (1968). The outward movement of the location of maximum axial velocity as D increases is evident, and while the secondary streamlines continue to manifest a vortex structure for $D = 606$, the beginnings of secondary and axial boundary layers are clearly discernable at the larger D value. This is more dramatically exhibited in Figure 4 for $D = 5000$, taken from Collins & Dennis, which shows also a much greater distortion of the secondary streamlines.

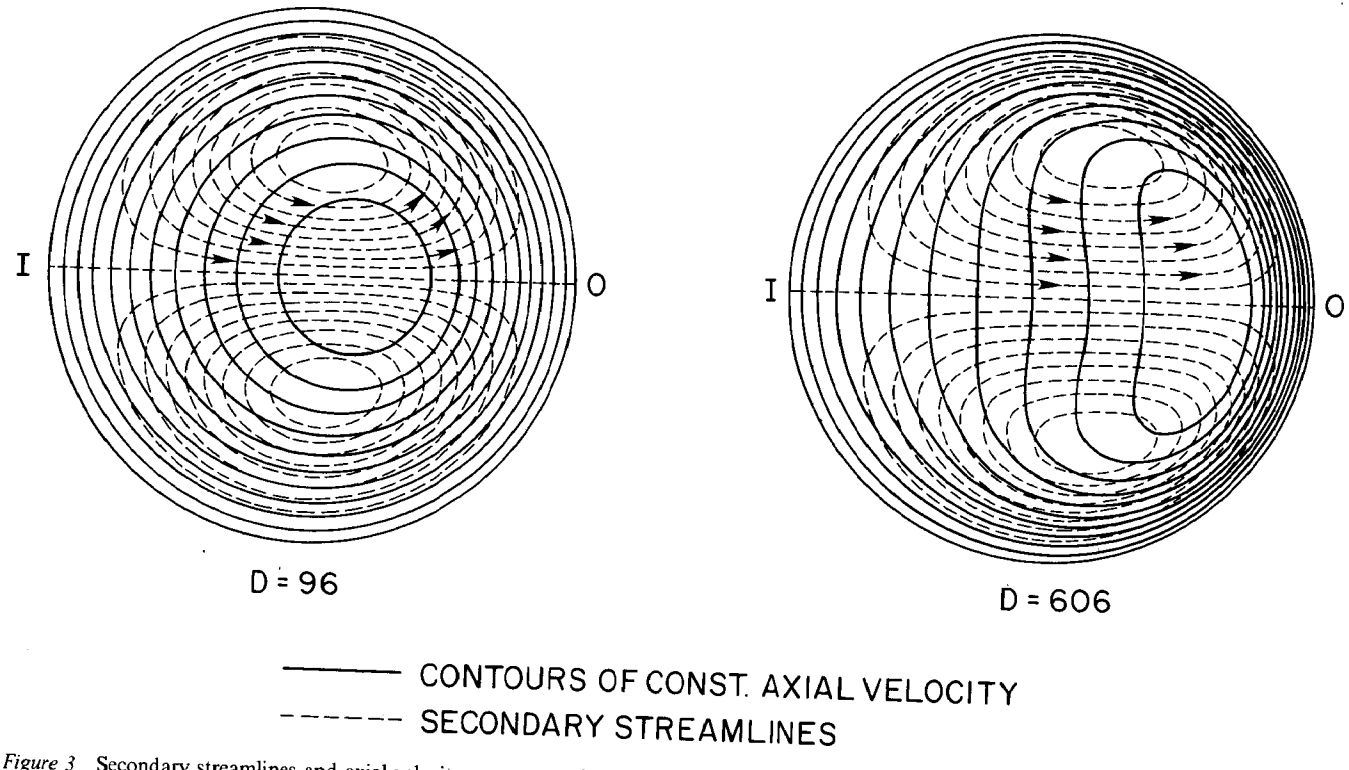

Figure 3 Secondary streamlines and axial-velocity contours at low and intermediate Dean numbers (McConalogue & Srivastava 1968). I denotes inner bend, O outer bend.

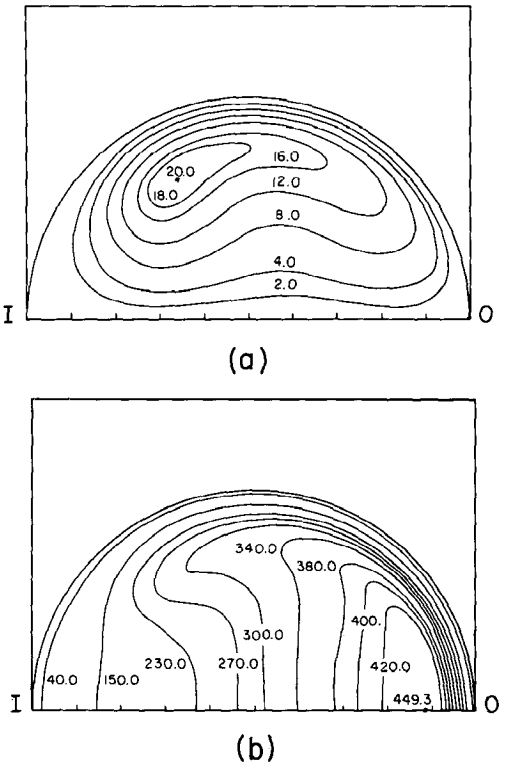

Figure 4 (*a*) Secondary streamlines and (*b*) axial-velocity contours at large Dean number, $D = 5000$ (Collins & Dennis 1975). I denotes inner bend, O outer bend.

A different approach was taken by Van Dyke (1978), who extended Dean's series by computer up to 24 terms and demonstrated that the series converges for $D < 96.8$. A Domb-Sykes plot and an Euler transformation was then employed to extend the series for λ_c/λ_s to $D = \infty$; the series agrees well with all the numerical solutions as well as the experimental data up to $\kappa \simeq 100$ (see Figure 7). This analysis predicts that

Table 1 Asymptotic friction ratio for large Dean number

λ_c/λ_s	Reference
$0.1064\,\kappa^{1/2}$	Adler (1934)
$0.09185\,\kappa^{1/2}$	Barua (1963)
$0.1080\,\kappa^{1/2}$	Mori & Nakayama (1965)
$0.1033\,\kappa^{1/2}$	Itō (1969)
$0.47136\,\kappa^{1/4}$	Van Dyke (1978)

λ_c/λ_s grows asymptotically as $\lambda_c/\lambda_s \sim 0.47136\kappa^{1/4}$, which, as is illustrated later, is at variance with all other existing solutions for large Dean numbers (see Table 1).

2.1.1.4 *Large Dean number* As the Dean number increases, the centers of the two vortices move to the outer bend, $\alpha = 0°$. There is a considerable reduction in flow in the curved pipe compared with a straight pipe. Adler (1934) observed that boundary layers exist on the two halves of the torus. His interpretation was that the two boundary layers, on the upper and lower halves, collide at the innermost point of the cross section, separate there, and form a reentrant jet that moves outward through the core. The boundary-layer model proposed indicates that λ_c/λ_s should be proportional to $\kappa^{1/2}$ (see Table 1), where $\kappa = (2a\overline{W}_0/\nu)(a/R)^{1/2}$. Subsequently, Barua (1963), Mori & Nakayama (1965), and Itō (1969) improved the boundary-layer model; they all found that $\lambda_c/\lambda_s \propto \kappa^{1/2}$. The coefficient of proportionality in this relationship differs slightly for different boundary-layer models (see Table 1). In Barua's model, the flow is assumed to consist of an inviscid core plus a thin boundary layer, with the additional assumption that the flow in the core lies in planes parallel to the plane of symmetry; this picture of the flow is not inconsistent with the numerical results of Collins & Dennis (see, for example, Figure 3, $D = 606$) discussed in the previous section. The Pohlhausen momentum-integral method is used to solve the boundary layer, which is coupled to the inviscid-core flow by assuming that the maximum circumferential velocity occurs at $\alpha = \pm 90°$. For a large D flow this assumption is not rigorously correct. Barua's integral solution indicates that the two circumferential boundary layers separate from the pipe wall about 27° away from the inner bend. This separation location according to Barua is in reasonable agreement with data of H. Squire (1954, unpublished) and Adler (1934). Itō also used the Pohlhausen integral method but with less restrictive conditions on the inviscid core. His model indicates that the fluid enters the secondary boundary layers within about 35° from the outer bend, i.e. $-35° \leqslant \alpha \leqslant 35°$; it also predicts that the boundary-layer thickness remains almost constant until it increases sharply in the neighborhood of the inner bend, $\alpha = 180°$. Itō's solution, however, unlike Barua's, does not predict separation.

It will be useful at this point to describe briefly how the flow pattern evolves as the Dean number increases. For small-Dean-number flows, the circumferential velocity attains its maximum value at $\alpha = \pm 90°$ and the two vortices are symmetric with respect to these values of α. As the Dean number increases, (secondary) boundary layers develop on the wall, with fluid entering these boundary layers near the outer bend and leaving near

the inner bend. Further increase of the Dean number, and hence the centrifugal force, leads to an increase in circumferential velocity and to more fluid being sucked into the secondary boundary layers near the outer bend. The secondary boundary layers adjust by thinning near the outer bend and thickening near the inner bend. Simultaneously, the locations of the maximum circumferential velocity move toward the outer bend. The two vortices are skewed by the adjustment of the secondary boundary layers. With further increase of the Dean number the secondary flow boundary layers near the inner bend thicken further, and according to some accounts (Barua 1963, Yao & Berger 1975), eventually separate, the width of the separation region gradually increasing for even larger D. No analytical model has yet been developed that includes the effect of this boundary-layer separation on the inviscid-core flow; more importantly, however, as has been mentioned above and will be further discussed below, the existence of this separation is very much in dispute. Interestingly, predictions of flow resistance by the various integral models, whether or not they predict separation, agree reasonably well among themselves and with the experimental data (see Table 1). This is probably because the viscous shear is small near the inner bend whatever the nature of the flow in this region and does not contribute much to the total flow resistance.

The interest in large-Dean-number curved-pipe flows has continued; however, in the past decade, far more attention has been given to finding the appropriate, consistent scales for each of the subregions of the flow field and to obtaining solutions, e.g. for the boundary layer, with greater precision than is possible using momentum-integral methods. We can only briefly sketch here these more recent developments; for a fuller account, see Pedley (1980).

We begin with the observation that the numerical results for intermediate D discussed in Section 2.1.1.3 suggest that the structure of the flow at large D is an inviscid rotational core surrounded by a thin boundary layer. If one seeks scales such that in the core inertia forces balance pressure gradients and in the boundary layer there is a balance between inertia, viscous, and centrifugal forces, then one finds that $w_{\text{core}} = O(D^{2/3})$, $\psi = O(D^{1/3})$, and the boundary-layer thickness is $O(D^{-1/3})$. (These scales are consistent with the numerical results of Collins & Dennis.) Using these scales, one can then obtain from (15) and (16) the governing equations for the core and the boundary layer. The core equation can be solved up to an arbitrary constant that can be determined by matching with the boundary layer. The equations for the boundary layer have been solved by Itō (1969) using a Pohlhausen momentum-integral technique, by Riley & Dennis (1976) using finite

differences, and by other investigators. All such solutions break down either at $\alpha = \pi$ or α considerably less than π. This is not necessarily due to separation of the boundary layer, because, for example, Itō does not predict separation, and local scaling arguments (Pedley 1980) suggest that the solution should be good up to $\pi - \alpha = O(D^{-1/8})$. Thus we are left with a number of open questions: (*a*) does the boundary layer extend right up to $\alpha = \pi$, and if so is there a collision of boundary layers at this point?; (*b*) is there an interaction of the boundary layer with the core near $\alpha = \pi$?; (*c*) does a reentrant jet form at $\alpha = \pi$ (see Section 2.2), and if so what is its effect upon the core? Some of these issues are addressed in the recent work of Stewartson et al. (1980) and Stewartson & Simpson (1982). Clearly, the flow structure at large D, and in particular the local structure and local shear variation near the inner bend, is not yet fully delineated and requires further study. This difficulty is not uncommon in other laminar flows at large Reynolds numbers. On the other hand, and on a more optimistic note, for correlating the flow resistance the available numerical solutions and boundary-layer models are probably sufficient, and have been verified by the experimental data.

2.1.2 FINITE δ It has already been pointed out that in general the flow in curved pipes depends on two parameters: the Dean number and the curvature ratio δ. While the influence of the latter has been studied much less than that of the former, it can play a major role in these flows.

Topakoglu (1967) solved (15) and (16) by expanding w and ψ in a double series in K [the Dean number defined by (24)] and δ, and obtained analytically the first few terms in the expansion. Larrain & Bonilla (1970) extended the double series to fourteenth order by computer. They studied the effect of curvature for $0 \leqslant \delta \leqslant 0.2$. The influence of δ is more profound for small K. For example, the percentage increment of the flow resistance for $\delta = 0.1$ can be seven times larger than that for $\delta \to 0$ at $K \simeq 18$. The absolute increment of the flow resistance increases with K for larger δ. The relative increment, however, diminishes rapidly when $K > 100$. Another interesting feature pointed out by Larrain & Bonilla is that the flow resistance is actually less than that in a straight pipe for a nonzero δ when K is about unity.

It is noteworthy that the series solution can be obtained for $\delta < 0.2$ and may not be valid for larger δ. The limit of small-Dean-number flow can be achieved by taking $\delta \to 0$ or $\mathrm{Re} \to 0$ if $\delta < 0.2$. That this is not the case for $\delta > 0.2$ suggests that the flow distribution for $\delta > 0.2$ may be quite different from that of Dean flow.

The boundary-layer models discussed in Sec. 2.1.1.4 were formulated in the limit $\delta \to 0$. Nunge & Lin (1973) reported Lin's (1972) extension of

Itō's model to study the effect of nonzero δ. Lin indicated that a significant δ-effect can appear when δ is as small as 0.07. A surprising finding is that the flow resistance for a strongly curved pipe, say $\delta = 0.5$, is less than that of a loosely coiled pipe, $\delta = 0.01$ when $K > 85$. Truesdell & Adler (1970) and Austin & Seader (1973) have solved (15) and (16) numerically, using relaxation methods, for small but finite values of δ ($\delta \leqslant 0.2$) and moderate values of Dean number. In contrast to the Lin result, the finite-difference solution of Austin & Seader shows that the flow resistance for $\delta = 0.2$ is slightly higher than that for $\delta = 0.01$. Despite the discrepancy of these two solutions for larger δ, they agree well for $\delta = 0.01$ over the range $100 \leqslant D \leqslant 400$. A comparison of Austin & Seader's solution with White's data for $0.0049 \leqslant \delta \leqslant 0.66$ shows that the variation of the flow resistance for $0.01 \leqslant \delta \leqslant 0.2$ falls within the scatter of the experimental data. The Truesdell & Adler and Austin & Seader solutions both demonstrate that the dependence of the flow resistance, and the flow in general, on δ is much smaller than that on K. The variation of λ_c/λ_s with δ seems to be no more than 10%, based on the limited available information for $\delta < 0.1$. On the other hand, it seems unlikely that a small-Dean-number flow can exist for large δ. We discuss this problem further in Section 4. Suffice it to say that a careful numerical study of (15) and (16) over a wider variation of δ for intermediate K would be useful in more fully establishing the importance of δ.

In his monograph on flow in the large blood vessels, Pedley extends existing theory, wherever possible, to nonvanishingly small values of δ.

2.1.3 HELICAL PIPES Although this fact is not always explicitly stated, almost universally the analyses described above are, strictly speaking, valid only for toroidally curved pipes. The question then arises as to whether the results of such analyses can be applied to helical pipes. Helical pipes have both a curvature and a torsion or twist, and therefore there is in addition to a (modified) Dean number a second independent parameter, a measure of the torsion. An early attempt to address this question was that of Truesdell & Adler (1970), who presented ad hoc quantitative arguments suggesting that their numerical solutions for a toroidally coiled tube were applicable to a helically coiled tube of moderate pitch if the radius of curvature of the toroidal tube was replaced by that of the helical tube. Wang (1981) and Murata et al. (1981) addressed this question more rigorously by obtaining, in a nonorthogonal helical coordinate system, solutions for steady, fully developed flow in helical pipes of small curvature. They both obtain analytic solutions for low Dean number and small torsion by successive approximation, and Murata et al. for larger Dean number and torsion by

numerical methods. Although Murata et al. are able to conclude, as suggested by Truesdell & Adler, that the resistance formula for a toroidally curved pipe is also applicable to a helically coiled pipe if the curvature of the helically coiled pipe is used in place of that of the toroidally curved one, their results and those of Wang show that there are significant differences, particularly in the secondary flow patterns, at very small and very large values of the (modified) Dean number.

Numerical solutions for arbitrary curvature ratios and finite pitch over the whole laminar-flow regime have been obtained by Manlapaz & Churchill (1980). They find the effect of pitch is significant only for coils for which the increase in elevation per revolution is greater than the radius of the coil. They also develop a correlating equation for the friction factor, or ratio, for all Reynolds numbers, all ratios of coil radius to tube radius, and all ratios of pitch to coil radius for which the flow remains laminar.

2.1.4 FINAL REMARKS In their continuing study of fully developed curved-pipe flow by numerical methods, Dennis and co-workers (Dennis & Ng 1982) again solved (15) and (16) for $96 < D < 5000$, but this time by Fourier-series expansion in α and series truncation of the resulting ordinary differential equations. For $D < 956$, Dennis & Ng find the usual symmetric pair of counterrotating vortices and their results fully agree with the earlier Collins & Dennis (1975) solution. The same type of solution is also found for $D > 956$, but in addition a second family of solutions sometimes emerges in which the secondary flow has a four-vortex pattern consisting of two symmetrical vortex pairs. This non-uniqueness, the existence of both a two-vortex and a four-vortex mode for a large enough value of D, had previously been reported (Masliyah 1980) for a curved pipe with semicircular cross section (the flat surface forming the outer bend). This dual four-vortex solution for a curved pipe with a circular cross section was discovered independently by Nandakumar & Masliyah (1982). Nandakumar & Masliyah show that bifurcation of the two-vortex solution into two- and four-vortex solutions at higher Dean numbers occurs for other cross sections as well. All of the above authors are in agreement that their results fall within the framework of the bifurcation theory of Benjamin (1978a, b). In each case they find the point at which the solution bifurcates into dual solutions in the manner suggested by Benjamin, from above, i.e. by *decreasing* the flow parameter, which in this case is the Dean number.

Interestingly, Dennis & Ng (1982) find that the values of the friction ratio λ corresponding to the four-vortex solutions are very close to those of the two-vortex solutions.

2.2 *Entry Flow*

As has already been pointed out, apart from a purely academic interest, the entry flow into a curved pipe is of great practical importance in that it informs us as to (*a*) the distance required for the flow to become fully developed, (*b*) the contribution of the entry region to the overall pressure drop, and (*c*) the sites of extrema in the wall shear. In addition, investigation of the flow development in the entry region might help to resolve some of the unsolved questions of the fully developed flow at large Dean number (see Section 2.1.1.4).

Whereas the entry flow in a straight tube or pipe has been extensively studied (see e.g. Schlichting 1979), the same cannot be said for a curved tube, no doubt in part because the fully developed flow is so much more complicated and even now is not fully investigated and understood.

We begin with a qualitative description of the development of the flow in a curved tube (Singh 1974, Yao & Berger 1975). When the fluid first enters the pipe from, say, a large reservoir the central core is not influenced by viscosity, the effects of which are confined to a thin layer near the walls. This boundary layer develops initially like that in a straight pipe. Thus, immediately downstream of the entrance the flow field consists of two regions: (*a*) an inviscid core in which the centrifugal force, due to the curved motion of the main body of fluid, is balanced by a pressure-gradient force directed toward the center of curvature; and (*b*) a thin boundary layer in which there is a balance between viscous and inertia forces. The inwardly directed pressure force acting on the core is impressed on the boundary layer, inducing a transverse, or azimuthal, flow in the boundary layer from the outside of the bend toward the inside. The displacement effect of the growing boundary layer accelerates the flow in the core, while the (second-order) azimuthal flow in the boundary layer induces a cross-flow from the inside to the outside of the bend. Thus the effect of curvature is to induce a secondary flow, with slower-moving fluid in the boundary layer on the wall moving inward, and faster-moving fluid in the core moving outward. The secondary boundary layer thus acts as a sink receiving fluid near the outer wall and a source of fluid near the inner wall.

The picture of the developing flow presented to this point is valid for all values of the Dean number up to a distance of $O(a)$ from the entrance. Beyond this point, the nature of the flow development depends on the Dean number. We defer consideration of this subsequent development of the flow, and first discuss the $O(a)$ region immediately downstream of the entrance, for which an analytical solution was given by Singh (1974). This solution is based on the observation that since

curvature effects are of second order in this $O(a)$ region, the solution can be obtained as a perturbation of the developing flow in a straight tube.

Singh begins with entry conditions (4a), corresponding to uniform total pressure, which requires that the static pressure behave as

$$p = -\tfrac{1}{2}(1 + \delta r \cos\alpha)^{-2}. \tag{28}$$

These entry conditions are exact solutions of the governing differential equations, (2); they therefore also represent the first-order solution in the inviscid core.

The first- and higher-order boundary-layer solutions and second- and higher-order core solutions are found by writing the solutions for these regions as double perturbation series in δ and β ($= \mathrm{Re}^{-1/2}$) about the straight-pipe solution and matching them using the techniques of matched asymptotic expansions. The analytic solution is given up to $O(\beta\delta)$, the lowest interaction term between tube curvature and the boundary-layer displacement effect.

Typical secondary-flow streamlines at different axial locations calculated from Singh's solution are shown in Figure 5. Initially there is an inward flow from the entire pipe circumference, due to the displacement effect of the boundary layer and resultant acceleration of the core flow, and, analytically, two singularities arise in the central region, a nodelike sink at the origin (point O) and a saddle-point-like stagnation point (point P); the latter singularity moves outward as the fluid moves downstream, eventually vanishing as the cross-flow becomes established.

One of the principal results of the Singh analysis is the prediction of a crossover in the location of the maximum axial wall shear, or skin

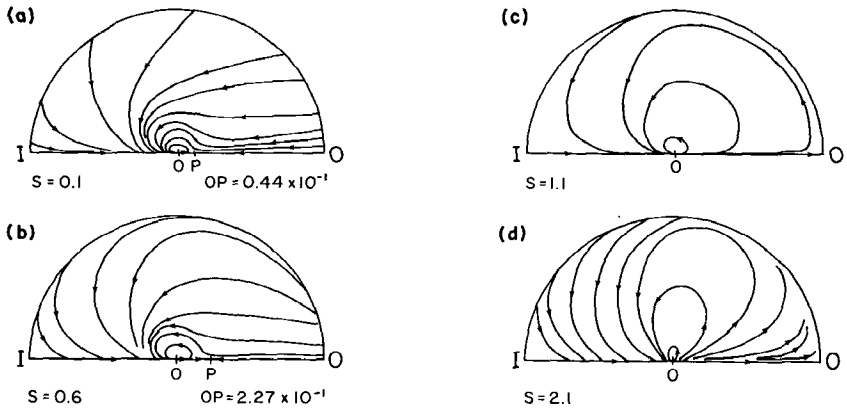

Figure 5 Streamlines in various cross-sectional planes near the entry in the developing flow in a curved tube (Singh 1974). I denotes inner bend, O outer bend.

friction, from the inner to the outer bend. The wall shear is larger initially at the inner wall because (*a*) the axial velocity is larger at the inner wall (since the initial profile is that of an inviscid vortex), and (*b*) the boundary layer is thinner there because of the shorter wall length, at the same s. A switch to the outer wall occurs at some location downstream of the entrance because (*a*) the point of maximum axial velocity moves outward, (*b*) the boundary layer is thinned at the outer wall because of the axial acceleration, and (*c*) the boundary layer is thickened at the inner wall and at the same time the external velocity decreases there. From the boundary-layer solution, the axial skin friction is found to be

$$\tau_{ws} = -\left(\frac{\mu\rho\overline{W}_0^3}{2as}\right)^{1/2}\left[0.4696 + \delta\cos\alpha(0.2562s^2 - 0.9392)\right], \qquad (29)$$

from which Singh calculates the crossover point to be located at $s \approx 1.9$ or $R\theta \approx 1.9a$, independent both of δ and β. This was verified experimentally by means of an electrochemical technique (Choi et al. 1979, Talbot & Wong 1982). The measurements, however, do suggest possibly some Reynolds-number effect, the crossover point moving slightly toward the inlet as Re increases, probably due to the boundary-layer displacement effect.

Singh shows that the solution for uniform-entry conditions, (4b), can be obtained by minor modification of the above solution for inviscid vortex entry. In this case the crossover occurs at $s \approx 0.95$, about half the value for the first case.

Beyond the distance $O(a)$ from the inlet, as mentioned above, the flow development depends on the Dean number. For small Dean number the centrifugal force, which is of second order in this initial $O(a)$ region, remains of second order as the fluid flows further downstream. The boundary layer continues to grow downstream, uneventfully, until it fills the tube and the flow is then fully developed, in a flow regime characterized by the axial length scale $a\mathrm{Re}$. Thus for a curved pipe at low Dean number, the entry length is of the same order as that in a straight pipe. The analytical solution for this flow region should be obtainable by perturbing the entry flow in a straight pipe and treating the secondary flow as a higher-order effect, in a manner similar to that of Dean (1928) for the fully developed flow.

Singh's solution breaks down when $s = O(\delta^{-1/2})$ [when a term of $O(s\delta^2)$ in the boundary-layer solution becomes of $O(1)$], or, dimensionally, $R\theta = O(a/\sqrt{a/R}) = O(\sqrt{aR})$. This is the point beyond which the curvature-induced centrifugal forces, initially small, become as important as inertia and viscous forces in the boundary layer, and because of the displacement effect upon the core flow, they become equally

important there as well. (Note that this means if $\delta \approx 0.2$, e.g. the maximum value in the aortic arch, Singh's solution is valid only for $s \lesssim 2$, about one diameter from the entrance.) Since $\sqrt{aR} = (a\,\mathrm{Re})/\kappa$, for $\kappa = O(1)$, $\sqrt{aR} = O(a\,\mathrm{Re})$ and the domain of validity of Singh's solution extends over most of the developing region, i.e. the flow essentially becomes fully developed before the centrifugal forces become important. For this case, then, the additional mixing due to the secondary flow appears to have little effect on the entry length, which is of the same order as that in a straight tube $[O(a\,\mathrm{Re})]$. For larger Dean number, one can develop a matched asymptotic expansion for the region $s = O(\delta^{-1/2})$ based on centrifugal forces being as important as viscous and inertia forces in the boundary layer. Such an expansion apparently breaks down (Singh, private communication) at a distance $R\theta = O(a\,\mathrm{Re})$, beyond which presumably the final transition to fully developed flow occurs.

For large Dean number the flow development is different. Centrifugal effects are as important as viscosity and inertia effects almost from the beginning. Much of the flow development occurs within a distance $O(\sqrt{aR})$, where these three forces balance, and since now $\sqrt{aR} \ll a\,\mathrm{Re}$, the entry length for this case is much shorter than that for a straight pipe. The magnitude of the secondary flow increases to the point that its displacement effect becomes larger than that of the axial flow. The cross-flow becomes stagnation-point-like near the outer bend. The convective effect of this locally stagnant flow prevents the secondary boundary layer from growing. Thus, the secondary boundary layer will remain thin, except possibly near the inner bend, as the flow asymptotically approaches the fully developed state (Barua-like flow; Barua 1963). The boundary layer near the outer generator acts as a reservoir, receiving the fluid moving toward the outer wall. The secondary boundary layers on the upper and lower halves of the tube either separate somewhat ahead of $\alpha = \pm 180°$ or collide at that point, forming an outwardly directed, or reentrant, jet.

Based on the above description of the flow, Yao & Berger (1975) have presented a model for the developing flow in a curved pipe for large Dean number. They derive two sets of equations; one for the inviscid-core flow and one for the three-dimensional boundary layer. They assume that the axial-velocity profile of the inviscid-core flow varies approximately linearly with distance from the vertical axis $\alpha = \pm \pi/2$, the coefficients of this linear expression being functions of axial distance down the pipe and determined from mass and momentum considerations and matching with the solution in the boundary layer. They also assume that the central cross-flow is essentially parallel to the plane of symmetry, an assumption employed by Barua (1963) for the fully developed flow and subsequently

confirmed for the developing flow by the numerical solution of Yeung (1980). The Kármán-Pohlhausen integral method is used to solve the three-dimensional boundary-layer equations with a uniform-inlet axial velocity. Yao & Berger find downstream of the region of distance $O(\sqrt{aR})$ from the inlet a third region of $O(\kappa^{1/2})$ where the developing flow approaches fully developed form[2]. Also, they show that the thickness of the fully developed boundary layer is $O(\kappa^{-1/2})$. This indicates that the axial flow is accelerated by a factor $1 + O(\kappa^{-1/2})$ due to the axial displacement effect. Due to the acceleration of the axial flow inside the boundary layer, the axial velocity of the inviscid-core flow slightly decreases in this region. Yao & Berger's integral solution of the three-dimensional boundary layer also predicts that separation of the secondary boundary layer occurs at an axial distance about $0.01\, a\cdot(\kappa/\delta)^{1/2}$ from the inlet. The width of the separation zone is found to grow downstream, asymptotically becoming approximately 54° wide (measured from the inner bend). Finally, their results show that the pressure drop in the entry region is less than the loss of pressure head necessary to maintain the fully developed flow, a consequence, perhaps, of the fact that the cross-flow in the entry region is smaller than that for the fully developed flow.

A careful comparison of Singh's boundary-layer equations, which are valid in $R\theta \sim O(a)$, with the three-dimensional boundary-layer equations of Yao & Berger valid in $R\theta \sim O(\sqrt{aR})$ reveals that Singh's equations are a special case of the latter for small secondary flow and are included in the latter equations in $R\theta \sim O(\sqrt{aR})$. Therefore Singh's solution is valid for $\theta \leqslant C_1\sqrt{\delta}$. The constant C_1 can in principle be determined by comparing Singh's solution with the solution of these boundary-layer equations in $R\theta \sim O(\sqrt{aR})$. Unfortunately, Yao & Berger's solution is too approximate to accurately determine C_1. Stewartson et al. (1980) numerically integrated the three-dimensional boundary-layer equations starting at the pipe entrance with the assumption that interaction between the boundary layer and the core flow is negligible in $R\theta \sim O(\sqrt{aR})$. They did not compare their solution with Singh's. However, Singh's solution indicates that the axial-velocity profiles at $\alpha = \pm 90°$ are not affected by the secondary flow in the region $R\theta \sim O(a)$. The numerical solution shows that this is true for $\theta \leqslant 0.3\sqrt{\delta}$, indicating that Singh's solution is valid for $C_1 = 0.3$.

The boundary-layer solution of Stewartson et al. (1980) for the developing flow was undertaken to clarify the nature of the fully developed

[2]Pedley (1980) demonstrates that this is the distance required for the transport of secondary vorticity from the boundary layer into the core.

flow for large Dean number (see Section 2.1.1.4). An interesting feature of their solution is the vanishing of the axial skin friction at $R\theta = 0.943a/\sqrt{\delta}$ at the inner generator, $\alpha = 180°$. Since both the circumferential velocity and the circumferential skin friction are no longer zero beyond this point, the authors conclude that the two secondary boundary layers collide here, and they conjecture that a radial jet is set up conveying fluid from the inner bend into the core region, the flow structure being much like that near the equator of a spinning sphere. The structure of the local singularity that occurs at this separation point of the axial boundary layer is explored further in Stewartson & Simpson (1982); considerable progress is made in elaborating this structure but only for points upstream of the separation point. Also, contrary to Stewartson et al., where the boundary-layer equations were integrated beyond the point of zero axial shear, Stewartson & Simpson conclude that the forward integration must stop at this point. To examine experimentally the behavior of the flow near this predicted collision point, Talbot & Wong (1982) measured the wall shear along $\alpha = 180°$ in a curved pipe of $\delta = 1/7$. They found that the wall shear dips to a minimum along this inner generator at a distance $0.96a/\sqrt{\delta}$ from the inlet, a location in good agreement with the numerical solution. Upstream of this point the predicted and measured wall shear stresses are also in good agreement; downstream of it, however, although both increase, there is substantial discrepancy between the measured values and those calculated (but now discounted).

Clearly, the nature of the developing flow in curved pipes for large Dean numbers is far from understood. The difficulty is primarily associated with the behavior of the boundary layers near the inner bend and with the interaction of these boundary layers with the core flow.

Before closing this section, we should mention the few fully numerical solutions for developing flow. Patankar et al. (1974) have applied their well-known finite-difference method to solve the "parabolized" Navier-Stokes equations for developing and fully developed flows in curved pipes. These equations were also solved numerically for this problem by Rushmore (1975). Using a finite-difference method of his own design, Liu (1976, 1977) has solved the full elliptic Navier-Stokes equations for one particular developing flow, flow into a 90° elbow from a reservoir of uniform total pressure, but for the fairly small Dean number $\kappa \approx 179$. Yeung (1980) has solved the entry-flow problem numerically for large Dean number by dividing the flow field into a boundary-layer region and an inviscid-core region. Notwithstanding the value of these solutions, they are still too crude to throw much light on the problem of the analytic structure of the developing, and fully developed, flow at large

Dean number, in particular near the inner generator. Ideally, for developing flow this would come from a fully three-dimensional solution of the full Navier-Stokes equations, with enough computational points to adequately resolve the thin wall boundary layers and the local structure near $\alpha = 180°$. The problem, akin to that for high-Reynolds-number finite-difference calculations, is how to do this in such a way that numerical viscosity does not "wash out" the details of this inner-bend flow structure.

Entry conditions Thus far we have mentioned at least three different entry or inlet conditions: (*a*) uniform total pressure, i.e. an inviscid vortex, (*b*) uniform axial velocity, and (*c*) straight-pipe Poiseuille flow. (In all three cases the radial and circumferential velocity components are taken to be identically zero.) Each of these has been employed as an inlet condition in experimental, analytical, and numerical investigations.[3] Strictly speaking, the inlet conditions can only be determined by solving the developing flow in the pipe simultaneously with the flow development before the fluid enters the pipe. The assumption of a profile at the entrance is then purely a pragmatic device, but necessarily only an approximate one, to avoid the necessity to deal with this obviously much more complicated flow situation. (For some indication of situations in which this simplified approach is inadequate, see Section 4).

Immediate to the inlet one would expect the flow development to depend on the choice of inlet conditions, so comparisons of different analyses or experiments for the developing flow in curved tubes is not always possible. This should not be a problem for the fully developed flow, which should be independent of (i.e. have "forgotten") the inlet conditions. The recent experimental results of Agrawal et al. (1978; see Section 8) indicate that whatever the configuration upstream of the entrance to the curved section, the flow very rapidly takes on a potential-vortex structure, before any flow development due to curvature occurs, so in future studies there is some reason to favor this as the inlet condition. It is interesting to note in this connection that in the numerical solution of Yeung (1980) the assumed uniform-entry profile developed into a potential vortex almost immediately downstream of the entrance.

Entry Length Of particular interest relative to curved pipe flows is the entry length, the length required for the flow to become fully developed, and its relationship to that for a straight pipe. For a straight pipe, the

[3] We note again that although this situation is not considered separately here, nonuniform velocity distributions at the entrance to a curved pipe can cause secondary flows to arise even in the absence of viscosity (Squire & Winter 1949, Hawthorne 1951).

entry length is commonly quoted as $l_s = 0.25a\,\mathrm{Re}$ (Fargie & Martin 1971), where $\mathrm{Re} = Ua/\nu$, and U is the uniform axial velocity at the entry to the pipe. Yao & Berger (1975) predict that at large Dean number the entry length in a curved pipe is $l_c = e_1(\kappa/\delta)^{1/2}a = e_1 a(2\,\mathrm{Re})^{1/2}\delta^{-1/4}$, where e_1 is weakly dependent on δ and Re lies between 2 and 4. Thus

$$\frac{l_c}{l_s} = 8e_1\kappa^{-1/2}, \tag{30}$$

so in the limit of very large Dean numbers, $l_c/l_s \ll 1$. For practical values of the parameters, however, this may not be the case; for example, if $\delta = 0.05$, $\mathrm{Re} = 2000$, then $\kappa = 894$, and $l_c/l_s = 0.584$, so the entry length is approximately half that for a straight pipe. Pedley (1980) has pointed out that there is at least partial experimental support for this functional dependence of l_c on Re and δ in the work of Olson (1971) and Agrawal et al. (1978). These investigators find the flow to be virtually fully developed at the last station measured: $s = 50$ for Olson, $s = 57$ for Agrawal et al; evaluation of $\mathrm{Re}^{1/2}\delta^{-1/4}$ for each of these yields 46 for Olson, 50 for Agrawal et al. Pedley also gives a physical argument supporting this scaling.

Finally, we note that the value of l_c predicted by Yao & Berger satisfies for large Dean number the inequality

$$\delta^{-1/2} \ll \frac{l_c}{a} \propto \mathrm{Re}^{1/2}\delta^{-1/4} \ll \mathrm{Re}, \tag{31}$$

where the rightmost expression represents the entry length in a straight pipe and the leftmost expression the range of validity of Singh's solution (1974).

3. UNSTEADY, LAMINAR FLOW IN A RIGID PIPE

Since flow in the aorta is pulsatile, and a description of flow in this blood vessel has been one of the prime motivations for much of the recent work on curved tubes, it is not surprising that a good part of this work has focused on the analysis of unsteady flow, although, as we shall see, with considerably less success than in the steady case. We are able here to do no more than give the briefest outline of this work, referring the reader to the relevant literature. As before we consider separately fully developed and developing flows, beginning with the former. Such studies may also have nonphysiological applications, e.g. in the analysis of fluidic devices, hydraulic control lines, etc.

3.1 *Fully Developed Flow*

3.1.1 OSCILLATORY FLOW We assume that the dimensionless pressure gradient p_s in (2d) varies as

$$-p_s = G + \bar{\alpha}^2 \hat{W} \cos \bar{\alpha}^2 t, \tag{32}$$

where G is the (constant) dimensionless steady component of the pressure gradient, ω the frequency of the oscillation, and $\hat{W}$ a characteristic velocity of the fluid that would result from the oscillation. We are also now replacing the nondimensionalizing velocity $\overline{W}_0$ in Equations (1) by ν/a. This means that time is now nondimensionalized with respect to the diffusion time a^2/ν. The parameter $\bar{\alpha}$, equal to $a\sqrt{\omega/\nu}$, is called the Womersley parameter in the blood-flow literature.[4]

If one assumes that the tube is loosely coiled, $\delta \ll 1$, Equations (2) again reduce so that a stream function can be defined as in (14), and one obtains as the governing equations, corresponding to (15) and (16),

$$\nabla_1^2 w' + D + \bar{\alpha}^3 (2R_s)^{1/2} \cos \tau = \frac{1}{r}(\psi_\alpha w'_r - \psi_r w'_\alpha) + \bar{\alpha}^2 w'_\tau, \tag{33}$$

and

$$\nabla_1^4 \psi + \frac{1}{r}\left(\psi_r \frac{\partial}{\partial \alpha} - \psi_\alpha \frac{\partial}{\partial r}\right)\nabla_1^2 \psi = -w' w'_y + \bar{\alpha}^2 \nabla_1^2 \psi_\tau, \tag{34}$$

where $y = r \sin \alpha$; $\tau = \bar{\alpha}^2 t$; D is the Dean number, defined as $D = (2\delta)^{1/2} G$; and R_s is a new dimensionless parameter, defined as $R_s = \delta \hat{W}^2/\bar{\alpha}^2$ or $\delta \hat{W}_a^2/\omega\nu$, where $\hat{W}_a = \nu \hat{W}/a$. [For compatibility with other studies, we have changed the definitions of nondimensional scaled velocities; instead of (6), the scaling now is $(u, v, w) \to (u, v, (2\delta)^{-1/2} w')$. We have, however, followed Pedley (1980), rather than many other investigators, in the notation and definitions, in particular that of $\bar{\alpha}$, because the connection with physiological flows of interest is more direct.]

We see from (33) and (34) that three independent parameters, D, $\bar{\alpha}$, and R_s, characterize these flows, and so there are a large number of possible flow situations. Since even a direct numerical treatment of these nonlinear equations for arbitrary values of the parameters would be formidable indeed, asymptotic analysis for different limiting cases is an attractive alternative; this has been done for a large number of cases by Smith (1975), only some of which are discussed below.

3.1.1.1 *Steady limit* This case corresponds to small perturbations about the steady flow; for small Dean number, it can be treated by a double

[4] We have followed standard notation in denoting the Womersley parameter by α, but with an overbar to avoid confusion with the azimuthal polar angle α.

series expansion in $\bar{\alpha}^2$ and D. For large Dean number, one must use boundary-layer ideas patterned after those described earlier for steady flow. For these analyses, see Smith (1975).

This steady limiting case, in which $\bar{\alpha} \ll 1$, is inappropriate for the flow in large arteries because there the values of $\bar{\alpha}$ are large and the amplitude of the oscillating component of the motion is at least as large as the mean component. Below we briefly consider flows in these situations, beginning with the case of purely oscillatory motion. For a much more complete account of this work, see Pedley (1980), from which the summary below borrows heavily.

3.1.1.2 *Zero mean pressure gradient: purely oscillatory motion* This case, for which G and hence D are zero, was first treated by Lyne (1971); it allows one to expose the effect of a purely oscillatory pressure gradient. For large $\bar{\alpha}$ the centrifugal forces cause a mean secondary flow to develop in the Stokes layer on the wall ($r = 1$), much like the steady streaming that develops in other high-frequency oscillatory viscous flows, which in turn drives steady secondary motions in the core. The flow in the latter region is governed by the "secondary-streaming Reynolds number" R_s, and can be analyzed analytically only in the limits of small and large R_s. For small R_s the core flow is a simple Stokes-flow problem, whereas for large R_s (the more physiologically relevant limit) the effects of viscosity are confined to thin boundary layers [of thickness $O(R_s^{-1/2})$] near the walls and along the plane of symmetry, the remainder of the core being inviscid and of uniform vorticity (of opposite sign in the upper and lower halves). The pattern of steady secondary streaming in the core, from the outside to the inside of the bend, predicted by Lyne in this large R_s limit, was also confirmed experimentally by him and Munson (1975).

A different approach to this purely oscillatory case was that of Zalosh & Nelson (1973), who linearized the Navier-Stokes equations by expansion in powers of an amplitude parameter, equal to $\delta \hat{W}^2$ in our notation and assumed to be small, and solved them by (numerical inversion of) finite Hankel transforms. The analysis is valid only for $R_s \ll 1$ but for all values of $\bar{\alpha}$. Closed-form solutions are obtained in the limits $\bar{\alpha} \to 0$ and $\bar{\alpha} \to \infty$. Claiming there to be a discrepancy between the equations and results quoted in Zalosh & Nelson, Mullin & Greated (1980b) have carried out an essentially parallel analysis using the same expansion and solution procedure. A closed-form analytic solution for this problem valid for *all* values of $\bar{\alpha}$ has been obtained by Zapryanov & Matakiev (1980).

3.1.1.3 *Nonzero mean pressure gradient* If D is not zero, but very small (i.e. $D \ll \bar{\alpha}^{-1} \ll 1$), the solution can be obtained as a power series in D,

with Lyne's solution the leading term (Smith 1975). For the large arteries, D is very large, and so are $\bar{\alpha}$ and R_s, e.g. in the canine aorta $D \approx 2000$, $\bar{\alpha} \approx 13$, and $R_s \approx 4200$. Because of the nonlinearity of the problem, the mean and oscillatory parts cannot be separated and one must simultaneously take D, $\bar{\alpha}$, and R_s to be large. Most relevant physiologically, in particular, is the ordering $1 \ll \bar{\alpha} \ll D < R_s$, with $D \ll \bar{\alpha}^3 R_s^{1/2}$, so that the amplitude of the oscillatory part of the pressure gradient is much larger than the mean; theoretically one would probably be most interested in the regimes in which transition occurs from outward secondary streaming in the core, characteristic of the steady pressure-gradient case, to inward streaming, characteristic of the purely oscillatory case. The only work done on this latter problem is that of Blennerhassett (1976), who studied cases for which $D \lesssim R_s$ in the limit $\bar{\alpha} \to \infty$. In this limit the Stokes layer, the thinnest layer on the wall, is the same as that calculated by Lyne (1971); hence one can focus on the steady component of the flow, which Blennerhassett shows can be determined from the solution of the steady equations (15) and (16), subject to boundary conditions (18), except that $\psi_r = 0$ is replaced by the slip velocity at the edge of the Stokes layer. In addition to some asymptotic results for this system, Blennerhassett obtains numerical solutions for general values of D and R_s. At not very large values of R_s and $D = O(R_s)$ the results are as expected, i.e. as D increases the flow pattern changes from one in which the secondary streaming is toward the inner wall and the peak axial velocity occurs near this wall (typical of purely oscillatory flow) to one in which the secondary streaming is toward the outer wall and the peak axial velocity occurs nearer that wall (typical of steady flow). Above some critical value of R_s, however, the situation becomes much more complicated, the volume flow-rate ratio Q_r (the mean flow rate in the curved tube divided by that in a straight tube at the same mean pressure gradient) becoming a multivalued function of D, implying that the flow at a given D depends on the nature of the approach to that state and the possibility of discontinuous jumps from one state of flow to another. For even larger values of R_s the situation appears to be still more complex, leading to the conclusion that the "problem of pulsatile flow in a curved tube is far from completely solved, even in the limit $\bar{\alpha} \to \infty$" (Pedley 1980).

Smith (1975) has reported on the little progress that is made if the limit $\bar{\alpha} \to \infty$ is not taken before any other limit, so that the Stokes layer is not necessarily the thinnest layer. In addition, he also treats asymptotically other limiting mean-pressure-gradient cases. (See also Blennerhassett 1976). Unfortunately, as noted by Pedley, for perhaps the most important application, the physiological one, not much headway has been made either asymptotically or numerically, in the former case because of the seeming intractability of the problem to such analysis.

3.1.2 GENERAL UNSTEADY FLOW Solutions for the oscillating flows discussed above, even if available for values of the parameters $\bar{\alpha}$, D, and R_s appropriate to the aorta, would not be fully appropriate for the flow in this vessel because δ is not vanishingly small and the pressure gradient is not of the form assumed in (32). More relevant treatments for flow in the aorta, assuming δ finite and a more realistic pressure-gradient waveform, the flow being assumed to start from rest, are given in the form of small t-expansions by Farthing (1977) and Pedley (1980).

3.2 *Developing Flow*

For very much the same reasons as for steady flow, one would like to know for an unsteady flow in a curved pipe how the flow evolves from the entrance profile to a fully developed structure far downstream.

Singh's (1974) analysis of steady flow very near the entrance, discussed in Section 2.2, can be readily extended to unsteady flow; this has been done by Singh et al. (1978). Assuming that the total pressure across the cross section at the entrance is constant, the entrance profile is then

$$u = v = 0, \qquad w' = \frac{W_0(t)}{1 + \delta r \cos\alpha}. \tag{35}$$

(It is also assumed that $W_0 \geq 0$ so there is no backflow.) This extension, using the same inlet profile, has also been carried out by Pedley (1980), who shows in addition how Singh's analyses (Singh 1974, Singh et al. 1978) may be modified so as not to require vanishingly small δ nor constant curvature, modifications important in the aorta. Again the solutions are given as series expansions and are obtained by matching the boundary layer on the walls to the core flow. Results are given both for the case when the flow is quasi-steady ($s\dot{W}_0/W_0^2 \ll 1$) and when it is not; we refer the reader to the original papers for a discussion of these results, and note here only the effect of the unsteadiness on the axial wall shear. The unsteadiness increases the skin friction during the accelerating phase ($\dot{W}_0 > 0$) through the accelerating pressure gradient, and decreases it during the decelerating phase ($\dot{W}_0 < 0$). Therefore the crossover of maximum shear (see Section 2.2) is inhibited in the acceleration phase (i.e. occurs at a larger value of s) and promoted in the deceleration phase. Since the effect of unsteadiness, or what Singh et al. call the entrance-velocity-fluctuation effect, on the skin friction increases as the flow develops further downstream, negative shear stresses, and therefore backflow near the wall, occur. During the accelerating phase the azimuthal skin friction falls below its steady value as s increases, perhaps ultimately becoming negative, but the range of validity of the series solution does not extend far enough to determine this.

The downstream extent of validity of this modified, unsteady, Singh series solution is the same as for the steady case (see Section 2.2).

Farthing (1977) has considered this problem when the curvature is slowly varying and has shown how, in an application to approximately quasi-static flow in the aorta, the small-s expansions of this section can be matched to the downstream diffusive flow, expressed as expansions in small t, referred to in Section 3.1.2.

For an experimental investigation of oscillatory flow development at the entry into a curved pipe, see Mullin & Greated (1980a).

3.3 *Final Remarks*

Numerical analyses of fully developed pulsatile flow are also presented in Rabadi et al. (1980), for small or large δ and a wide range of $\bar{\alpha}$ and D, and in Lin & Tarbell (1980). For experimental studies of pulsatile and oscillatory curved-tube or pipe flows, see Chandran et al. (1979), Chandran & Yearwood (1981), Lin & Tarbell (1980), Munson (1975), Mullin & Greated (1980a,b), and Talbot & Gong (1982).

4. FINITE BEND

Short segments of curved pipe, finite elbows, are ubiquitous and indispensible components in piping systems. The flow in a finite elbow is almost always a developing flow. Because of its importance in engineering applications, and its unique feature of changing the flow structure in the straight-pipe sections upstream and downstream of the elbow, we single it out from our previous discussion and use it as a vehicle to discuss the possible inlet conditions for a curved pipe in general.

Itō (1960) carried out an exhaustive set of measurements of the pressure losses in smooth-pipe bends for various elbow angles. Two long straight pipes were connected to the elbow. (Straight-pipe sections upstream and downstream of the elbow long enough for the establishment upstream and reestablishment downstream of Poiseuille flow eliminate the unknown influence of the inlet and exit conditions on the flow development in the elbow.) A typical plot of the pressure distribution in a 90° elbow system is given in Figure 6. Although the data in this figure are for a Reynolds number corresponding to turbulent flow, the general characteristics are equally relevant to laminar flow. The dramatic pressure variation near the inner and outer bends of the elbow is associated with the existence of the secondary flow. The most interesting feature of this figure is that the pressure drop starts to deviate from that of a Poiseuille flow 5–10 diameters upstream of the inlet of the elbow, the maximum pressure deviation occurring about 45° into the 90° elbow. At

the inlet the pressure deviation is about 40–50% of its maximum value, at the exit about 20–40% of its maximum value. The pressure gradient gradually approaches that of a Poiseuille flow in the downstream straight section about 40–50 diameters from the elbow exit; for laminar flow the influence of the bend on the downstream flow almost certainly extends further. Thus, when a curved section of pipe is connected to straight sections very significant disturbances are communicated both upstream and downstream, from the curved into the straight sections and vice versa. Although the secondary flow may not reach its fully developed state in Itō's experiments because the elbow is short, the measurements indicate that a substantial secondary flow develops before the fluid enters the elbow, and that the secondary flow decays sharply before the fluid exits the curved section. The data also show that the flow development in the elbow is not a function of θ, the elbow angle, but depends on $\theta/\sqrt{\delta}$. Itō's measurements were for bends of circular cross section; for bends of rectangular cross section, see Ward-Smith (1968).

This discussion of short circular-arc bends has necessarily been brief. For a fuller discussion, see Ward-Smith (1980).

Having gained some appreciation of the "upstream effect" of a curved pipe, we now discuss briefly the inlet condition when such a pipe is

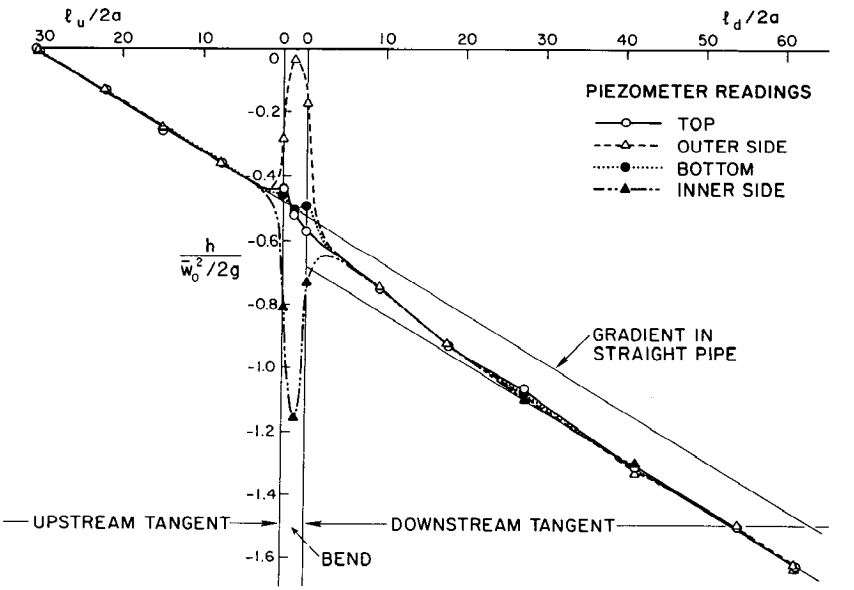

Figure 6 Pressure distribution along a 90° pipe bend and upstream and downstream connecting straight-pipe sections (Itō 1960). $R/a = 3.7$, $\mathrm{Re} = 2\times10^5$, h = head loss, l_u = length of upstream tangent, l_d = length of downstream tangent.

connected to a large vessel. Uniform axial velocity, the most common idealized inlet condition, is generated by the sudden contraction of the fluid passage. A strong favorable pressure gradient thins the boundary layer and results in an almost uniform axial-velocity profile. This has been measured by Agrawal et al. (1978). Apparently, the "upstream effect" is suppressed by the strong acceleration induced by the sudden contraction. On the other hand, the measured "crossover" point (see Section 2.2) agrees with Singh's solution with an assumed irrotational inlet flow condition. Strictly speaking, the inlet condition should be determined by simultaneously solving for the flows in the large vessel and the downstream curved pipe. Smith (1976b) studied the flow development in a straight pipe followed by a slightly coiled pipe. He treated the upstream effect by a coordinate transformation and neglected the dominant effect of geometric change, which is transmitted upstream via pressure disturbance. There is no other analytical (or numerical) treatment available.

Before closing this section, we briefly return to our discussion of the role δ plays in determining the general characteristics of curved-pipe flows. It has been demonstrated that the detailed geometric effects, represented by the terms multiplied by δ in Equations (8), contribute little to change the flow structure, at least for $\delta \lesssim 0.2$. This justifies the assertion that the limit $\delta \to 0$, $\delta^{1/2}\mathrm{Re}$ finite, of (8) indeed yields all the possible flow patterns for δ small but not necessarily infinitesimal. Functionally, then, the local shear depends only on Dean number, its coefficient varying weakly perhaps with δ. A good example of what can happen when δ is not small is a 180° elbow with $\delta = 1$. The axial flow may separate at the inner bend for very low Reynolds number, say $\mathrm{Re} \sim 10$, corresponding to $D = \sqrt{10}$, a small Dean number, but the flow pattern differs completely from small-Dean-number flow, suggesting that one must exercise great care when using the existing solutions for curved-pipe flows for small D when δ is not also small.

5. DIFFERENT GEOMETRIES, WALL CHARACTERISTICS, AND FLUID PROPERTIES

5.1 Different Cross Sections

Solutions have been obtained for steady fully developed flow in curved pipes of other than circular cross section. For low Dean number and a smooth, symmetric cross-sectional contour, such extensions would appear to present primarily mathematical difficulties. For an elliptic cross section and small curvature, Itō (1951) obtained, by successive approxima-

tion, the solution to second order in Dean number. Apparently unaware of this work, Cuming (1952) independently obtained the solution to first order, and Srivastava (1980) to second order. Srivastava's analysis is valid for larger curvature in that, following Topakoglu (1967) for a circular cross section, his solution is in the form of a double series expansion in Reynolds number and curvature ratio; he also gives explicitly an expression for the effect of curvature on flow resistance or the flux in the pipe. Numerical solutions for small but finite curvature ratio and moderate values of Dean number for an elliptic cross section have been obtained by Truesdell & Adler (1970). All of these solutions assume symmetric orientation of the elliptical cross section, i.e. that the axes of the ellipse are parallel and perpendicular to the symmetry plane of the pipe ($\alpha = 0$). For an elastico-viscous liquid Thomas & Walters (1965) obtain the solution, to first order in Dean number, for an elliptic cross section, the axes of which are arbitrarily oriented with respect to the symmetry plane.

Curved pipes of rectangular cross section are used extensively in industrial applications, in particular in heat- and mass-transfer apparatus, so considerably more work has been done on this cross section, both theoretically and experimentally. Itō (1951) and, for a square cross section, Cuming (1952) obtained solutions to first order in Dean number by successive approximation. Mori & Uchida (1967) obtained for a square cross section asymptotic solutions for large Dean number based on the boundary-layer approximation. Spanning the Dean-number range, from small to intermediate to fairly large values, and a wide range of cross-sectional aspect ratios, there are the numerical solutions of Cheng & Akiyama (1970), Cheng et al. (1976), and Schilling & Simon (1979). In their numerical solutions for a square cross section, Joseph et al. (1975) found that the expected secondary flow pattern with twin counterrotating vortices occurs at low Dean numbers, whereas at higher Dean numbers four secondary vortices, counterrotating in pairs, are present. The normal twin counterrotating secondary vortices are also present but are distorted to accommodate the additional pair of vortices, which are symmetrically located near the outer wall above and below the symmetry plane; though smaller than the normal vortices, they are equally strong in velocities. These four-vortex solutions for large Dean numbers were subsequently found for rectangular cross sections by Cheng & Akiyama and Cheng et al.

Dean & Hurst (1959) obtained approximate analytic solutions for flow in curved pipes of rectangular and circular cross sections assuming the secondary flow is a uniformly moving stream, from the inner to the outer bend.

To obtain analytic solutions for a general cross section at large Dean number, one can use boundary-layer ideas like those discussed in Section 2.1.1.4 and the situation is more complicated than that for low Dean number. Smith (1976a) has considered this problem and presents an asymptotic description for a general symmetric section. An explicit solution is presented for a triangular cross section. Solutions for flow in a triangular cross section have been obtained numerically for a wide range of Dean numbers by Collins & Dennis (1976a,b). For a rectangular cross section Smith puts forward analytical and numerical arguments that point fairly conclusively to the nonexistence of an attached laminar flow, near the inner bend at least. Humphrey et al. (1977) have numerically solved the Navier-Stokes equations for a strongly curved 90° bend of square cross section connected to upstream and downstream straight sections. They also assess the extent to which reduced, such as "parabolized," forms of the full equations can be utilized to describe the flow.

Nandakumar & Masliyah (1982) have studied general curved cross sections by solving the full Navier-Stokes equations numerically in a bipolar-toroidal coordinate system. They find that bifurcation of the two-vortex solution into two- and four-vortex solutions at large Dean numbers exists irrespective of the shape of the cross section. The procedure for obtaining these dual solutions and the explanation of their origin comes from the work of Benjamin (1978a,b).

5.2 *Variable Curvature*

Murata et al. (1976) have analyzed theoretically the steady fully developed low-Dean-number flow through curved pipes of circular cross section and variable curvature, the center of curvature being assumed to lie along a specified two-dimensional curve. Pulsatile flow in such a pipe was considered by Inaba & Murata (1978). Pedley, in his account of the flow in curved pipes, extends existing theory, where possible, to account for the effect of nonuniform curvature.

5.3 *Flexible Walls*

Because sites of curvature, which occur frequently in the arterial system, are often also sites of atherosclerotic involvement, fluid-dynamic phenomena have been suggested as a causative factor in atherogenesis. A number of hypotheses for such a causal relationship have been put forth, beginning with that of Texon (1960), who implicated the "pulling" or suction effect on the intima of the low-pressure region near the inner bend, followed by Fry (1968), who suggested it was damage done to the

endothelial cell lining in regions of high wall-shear stresses, then by Caro et al. (1971), who suggested a shear-dependent mass-transfer mechanism that implicated regions of low wall shear as being most dangerous. The resultant controversy, still unresolved (Nerem & Cornhill 1980), would obviously benefit from the availability of as complete a model of arterial flow as possible. To this end, Chandran et al. (1974) have presented an analytical model of fully developed oscillatory flow of a viscous incompressible fluid in a thin-walled elastic tube. The formulation and analysis are closely patterned after those of Morgan & Kiely (1954) and Womersley (1957) for oscillatory flow of a viscous fluid in a straight elastic tube; in fact, theirs is a perturbation of these analyses, assuming the curved tube to be of small curvature. The governing equations for the fluid and the thin elastic-tube wall (shell equations) are linearized, assuming (*a*) small radial wall displacements, (*b*) small a/λ, where λ is the wavelength of the pressure wave, (*c*) small w/c, where w is some characteristic axial velocity and c is the wave velocity, and finally (*d*) small δ. Only purely oscillatory motions are considered, the results showing that the secondary motions in the core are toward, and the peak axial velocity shifted to, the inner wall, both contrary to the case of steady flow and in agreement with the work of Lyne (1971) for rigid tubes. The wall shear is, again in contrast to steady flow, higher at the inner wall. Since arterial blood flows are subject to pulsatile pressure gradients with nonzero mean and many modes, the actual wall-shear distributions will depend on the relative importance of the steady- and oscillatory-flow components. In Chandran et al. (1979), these components are compared for a typical large curved artery and a typical extracorporeal device (a coiled-tube membrane oxygenator). Such comparisons, or indeed superpositions, of the steady and oscillatory components are often employed in arterial-flow analyses (McDonald 1974), but since they assume no interaction between these components they should be approached with caution (see Pedley 1980; also Section 3.1.1.3).

In addressing the question of the applicability of the unsteady, rigid-tube analyses of Section 3 to flow in the aorta, it should be pointed out that while wall distensibility is particularly important in propagation of the pulse wave and determining the local pressure gradient, it is less important in determining the fluid motion because λ is large compared with the length of the ascending aorta and w/c is small (Lighthill 1975).

5.4 *Porous Tubes*

Zapryanov & Matakiev (1980) have analyzed for a slightly curved porous tube the same unsteady problem considered for a nonporous tube by

Zalosh & Nelson (1973) and Mullin & Greated (1980b), namely the flow due to a purely oscillatory pressure gradient of small amplitude. They obtain a closed-form analytic solution valid for all values of the frequency parameter $\bar{\alpha}$.

5.5 *Non-Newtonian Fluids*

There have been extensions for a curved pipe of circular cross section of the original steady, fully developed, low-Dean-number analysis of Dean (1928) to non-Newtonian fluids. Among these are the work of Jones (1960) for a visco-inelastic, Reiner-Rivlin fluid; Kamel & Kaloni (1977) for a Cosserat fluid; Thomas & Walters (1963, 1965), the latter of these for an elliptic cross section, and Sharma & Prakash (1977) for a second-order viscoelastic fluid; and Jones (1967) for a third-order Coleman-Noll fluid. Questioning the adequacy of such second- or third-order fluid models at rates of deformation likely to occur in practical curved-pipe flows, Mashelkar & Devarajan (1976a) analyzed, for large Dean numbers, the flow of a power-law fluid using the momentum-integral approach of Itō (1969).

A number of papers have analyzed heat transfer in curved-pipe flows for non-Newtonian fluids. Raju & Rathna (1970) did so for a power-law fluid and found that dilatant fluids would be more efficient for the working of heat exchangers, while Srivastava & Sarin (1973a,b) did likewise for an elastico-viscous fluid for both circular and elliptic cross sections, for the latter case using the solution for the velocities obtained earlier by Thomas & Walters (1965). For unsteady flow, James (1975) has extended the analysis of Zalosh & Nelson (1973) for periodic pressure gradients to the case of an elastico-viscous liquid, in particular to study the effect of elasticity on the "negative centrifuging effect" discovered by Lyne (1971; see Section 3.1.1.2).

Measurements of friction factors for the flow of non-Newtonian fluids in curved pipes have been reported by Mishra & Gupta (1979), Singh & Mishra (1980), and Mashelkar & Devarajan (1976b), the last of these finding a "drag reduction" effect for viscoelastic fluids that could be correlated in terms of a Weissenberg number. Tsang & James (1980) noted that polymer additives caused a reduction of the secondary motion in curved tubes. Finally we might note a different application of such experiments in the work of Hayes & Hutton (1972), who used measurements of streamline patterns produced by flows in curved tubes and a third-order simple fluid model to determine the sum of the first and second normal-stress coefficients.

5.6 *Multiphase Flow*

Gould et al. (1974) have obtained correlations for predicting pressure distributions for two-phase flows. Morimoto & Ousaka (1974) did measurements on the effect of a 180° curved-pipe bend, through which an air-water mixture is flowing, on the flow in the upstream and downstream straight-pipe sections. Measurements of the same two-phase mixture flowing in bends of various curvatures and angles following straight-inlet conditions were carried out by Maddock et al. (1974), on the basis of which they suggested a flow structure for the developing region of a bend.

For more recent experimental work, plus references to other work in this area, see Whalley (1980). For the effect of curvature on boiling see Jensen & Bergles (1981, 1982).

6. MIXING AND MASS TRANSPORT IN CURVED TUBES

6.1 *Laminar Dispersion*

Erdogan & Chatwin (1967; see also Erdogan 1968) analyzed the effect of curvature on laminar dispersion of solute injected into a curved circular tube through which a solvent is in steady laminar motion. Using the velocity distribution obtained by Dean (1927, 1928), they show that the classical Taylor-Aris theory for a straight pipe is valid for a uniformly curved tube, and derive an expression for the diffusivity that predicts that for all common liquids and most gases the diffusivity is reduced by the curvature. McConalogue (1970) has also considered this problem when molecular diffusion is negligible and convection is the dominant dispersion mechanism, employing as velocity distributions those obtained by him and Srivastava (McConalogue & Srivastava 1968) for higher Dean number. He also found the axial dispersion to be lower than that in a straight tube. Nunge et al. (1972) reconsidered the general dispersion problem analytically, using instead the velocity distributions obtained by Topakoglu (1967) so their solution was not limited to small values of the curvature. Their results, in contrast, predict that the dispersion coefficient may be significantly increased by curvature at low Reynolds numbers, particularly in liquid systems of biological interest. Experiments measuring laminar dispersion in curved tubes and the conditions under which the Taylor-Aris theory is applicable to such tubes have been reported by Caro (1966) and Nigam & Vasudeva (1976). In an experi-

mental investigation of the use of the indicator dilution bolus-injection technique to measure flow parameters in curved tubes, Patel & Sirs (1977) found flow-rate estimations are more reliable than those of straight tubes due to secondary flows tending to disperse the indicator uniformly over the vessel cross section.

6.2 *Mass Transfer*

There are a number of interesting studies of the effect of tube curvature on mass transfer, covering a wide area of potential applications. Nunge & Adams (1973) describe, for desalination purposes, a new design for reverse osmosis in a curved-tube system, utilizing a split membrane over the circumference to take advantage of the scouring-silting nature of the secondary-flow pattern. Earlier, in an analytic study, Srinivasan & Tien (1971) found a significant increase in the mass-transfer rates in reverse osmosis due to the tube curvature. In an experimental study of condensation of water vapor from moist air in curved rectangular ducts, Smol'skiy & Chekhol'skiy (1978) found that heat- and mass-transfer rates and pressure drop were significantly higher than in straight channels. Since in membrane oxygenators the primary resistance to gas transfer comes from the blood boundary layer adjacent to the membrane, the induction of secondary flow, and therefore additional mixing, by curvature of the blood channel had been suggested almost from the beginning of the use of these devices (Weissman & Mockros 1968). Among the more recent work along these lines is that of Tanishita et al. (1978; see also Richardson et al. 1975), who report and study a new design of artificial membrane oxygenator consisting of curved tubes with periodically varying curvature wound in woven patterns. They find an augmentation in gas-transfer performance due to tube curvature similar to that found for helically coiled tubes but with lower flow resistance.

6.3 *Flow of Fluid-Particle Mixtures*

There have been a number of investigations of the motion of fluid-particle mixtures in curved tubes. Kaimal & Devanathan (1980) obtained trajectories of particles in such a flow for small δ as an asymptotic expansion in powers of Dean number. Yalamov & Muradyan (1980) obtained trajectories and capture coefficients of aerosol-particle mixtures in curved channels. In a theoretical investigation of diffusional deposition in a curved tube, Shaw & Rajendran (1977) showed that the secondary swirling motion in such a tube would increase diffusional deposition of airborne particles in the curved bronchial airways of the human respiratory tract. Yeung (1979) investigated analytically the motion of gas-

particle mixtures in curved pipes to obtain information about impact velocities, and impingement angles and mass fluxes, quantities of particular interest in assessing pipe erosion in such flow systems. Jain & Prabha (1982) analyzed gas-particle flow in slightly curved pipes of circular and rectangular cross sections assuming, following Dean & Hurst (1959), a uniform outward streaming for the central portion of the cross section.

7. THERMAL EFFECTS

Extensive studies have been made of convective heat transfer in coiled pipes and finite elbows, because of their practical applications in heat exchangers. A variety of the flow models discussed earlier as well as full numerical approaches have been used to predict the heat-transfer rate. Representative papers are Akiyama & Cheng (1974), Berg & Bonilla (1950), Dravid et al. (1971), Hausen (1943), Janssen & Hoogendoorn (1978), Kalb & Seader (1972, 1974), Kubair & Kuloor (1966), Mori & Nakayama (1965, 1967), Oliver & Asghar (1976), Owhadi et al. (1968), Patankar et al. (1974), Schmidt (1967), Seban & McLaughlin (1963), Shchukin (1969), Simon et al. (1977), Singh & Bell (1974), Tarbell & Samuels (1973), and Zapryanov et al. (1980). The outstanding feature of convective heat transfer in curved pipes is that, due to the additional mixing by the secondary flow, the mean heat-transfer rate is larger than that in a straight pipe at the same flow rate. The local Nusselt number attains its maximum at the outer bend due to the local stagnation-like flow, and its minimum at the inner bend due to the reverse stagnation-point-like flow. Effects of natural convection have, however, not been considered in the literature cited above. Abul-Hamayel & Bell (1979) deduce from their experiments that the maximum Nusselt number does not always occur at the outer bend for a horizontal curved pipe. Yao & Berger (1978) obtained a series solution for a fully developed flow for small Dean number and the product $\mathrm{Re}\,\mathrm{Ra}$, where Ra is the Rayleigh number. For a horizontal curved pipe the centrifugal and buoyancy forces combine to yield two skewed vortices, which may be viewed as the superposition of two "horizontal" vortices induced by the centrifugal force and two "vertical" vortices induced by the buoyancy force. Consequently, the stagnation-point-like flow moves from $\alpha = 90°$ to somewhere between 0° and 90°, where the maximum Nusselt number occurs. Prusa & Yao (1982) obtained a finite-difference solution for larger D and $\mathrm{Re}\,\mathrm{Ra}$. The location of the local maximum axial shear predicted by the series solution agrees well with that by the finite-difference method for the whole range of D and $\mathrm{Re}\,\mathrm{Ra}$. This may be because the location of the maximum axial shear (or Nusselt number) is determined by the ratio of

D to ReRa, centrifugal force to buoyancy force, and not by their individual values.

Prusa & Yao compared the mass-flow rate in a heated curved pipe with that in a straight pipe under the same axial pressure gradient and found that large overheating can enhance the secondary flow, increase the flow resistance, and reduce the flow rate. Consequently, a heated curved pipe can be a poorer heat-transfer device than a straight pipe under the same axial pressure gradient. A flow-regime map is provided to determine when one should consider the effect of buoyancy force. The results of analyses that do not consider the effect of buoyancy can be assumed valid only when ReRa is very small compared with D.

8. EXPERIMENTAL STUDIES

The literature on experimental studies of curved-pipe and duct flows is extensive, and space limitations permit only a few representative investigations to be described, some of which already have been mentioned. References to additional work may be found in the literature cited.

The primary emphasis of the early experimental work on the flow in curved pipes of circular cross section was on measurements of the friction factor, or ratio, λ_c/λ_s, defined [see the paragraph above (21)] by White (1929) as the ratio of the resistances in a curved and straight pipe carrying the same flux. In Figure 7, friction ratios measured by White (1929), Adler (1934), and Itō (1959) are plotted as a function of the Dean number κ for different curvature ratios $\delta(=a/R)$, ranging from loosely coiled to more tightly coiled pipes. The departure of each curve for fixed δ from the envelope of experimental points, the κ at which this occurs increasing as δ increases, is usually ascribed to the onset of turbulence. For small Dean number and small δ, the series (21) obtained by Dean (1928) agrees very well with the experiments. For larger κ the envelope of experimental points, before the onset of turbulence, is well-fitted by the expression $\lambda_c/\lambda_s = 0.0969\kappa^{1/2} + 0.556$, proposed by Hasson (1955) to correlate White's data in the range $30 < \kappa < 2000$. This square-root variation wth κ is predicted by all the boundary-layer analyses (see Section 2.1.1.4 and Table 1), with coefficients of proportionality that differ only slightly from one another and Hasson's correlation. The finite-difference calculations (see Section 2.1.1.3) agree well with the experiments for low and intermediate κ for all the values of δ shown, and tend toward the boundary-layer results for larger κ. For example, Collins & Dennis (1975) fit their finite-difference solution to $\lambda_c/\lambda_s = 0.1028\kappa^{1/2} + 0.380$. Also shown in Figure 7 is Van Dyke's (1978) asymptotic series ($\kappa \to \infty$) result $\lambda_c/\lambda_s \sim 0.47136\kappa^{1/4}$, obtained by his extension of Dean's

series; this agrees well with the experimental data for $\delta \leqslant 1/250$ over much of the laminar range of κ, but diverges from the experimental data and the finite-difference and boundary-layer solutions for $\kappa \gtrsim 100$ when the coiling is tighter. Van Dyke suggested that this discrepancy was due to the inaccuracy or incorrectness of the then-available numerical and analytic solutions, but this contention has been weakened by later more refined numerical calculations (Dennis 1980). Neither can the subsequent discovery of the bifurcation, at large Dean numbers, of the two-vortex solution into two- and four-vortex solutions (Section 2.1.4) account for the discrepancy, since, as found by Dennis & Ng (1982), the friction ratios for the dual solutions are nearly the same. However, it is possible, as these latter authors suggest, that Van Dyke's asymptotic series solution is yet a third solution.

Adler also made extensive Pitot-tube measurements of axial-velocity distributions in fully developed steady laminar flow in curved circular pipes. His results exhibit clearly the now well-known skewing of the axial-velocity maximum toward the outer wall of the bend. Less complete data are available for the axial-velocity distributions in fully developed turbulent flow, but the results are similar to those of laminar flow.

More recent work has focused on developing flows in curved pipes and ducts, with inlet conditions being either an essentially inviscid, flat velocity profile such as is produced by a bell-mouth entry from a large chamber, or a fully developed straight-pipe velocity profile. The availability of laser velocimetry has made possible the measurement not only of the axial-velocity profiles, but also the profiles of the secondary motion, usually the component parallel to the plane of curvature but in a few instances the component perpendicular to this plane as well.

Agrawal et al. (1978) have measured axial- and secondary-velocity distributions in 180° curved circular pipes under steady laminar flow and

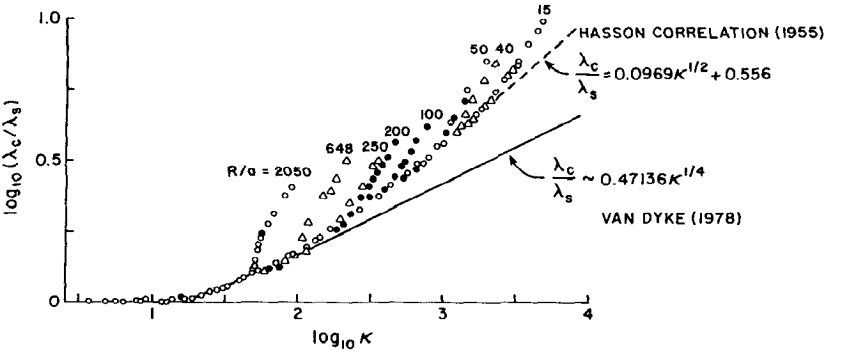

Figure 7 Friction ratios for various curvature ratios. ○, White (1929); ●, Adler (1934); △, Itō (1959) ($\kappa = 2D = (2a\bar{W}_0/\nu)(a/R)^{1/2}$). From Van Dyke (1978).

bell-mouth entry conditions for κ ranging from 138 to 679. Some of their principal findings are now described briefly.

The axial-velocity profiles very close to the entry of the curved section are found to have a potential-vortex structure, with the velocity maximum located in the neighborhood of the inner wall. With flow development, this inner-wall maximum is eroded by the action of the outwardly directed secondary flow in the core fluid, and the axial-velocity profiles are gradually transformed into the outwardly skewed, fully developed forms. At the lowest Dean number this transformation occurs in a relatively smooth fashion, but for $\kappa > 500$, doubly peaked axial-velocity profiles are found within the flow-development length. The value of κ at which doubly peaked axial velocity profiles first make their appearance is not accurately known, but is estimated to be in the neighborhood of 300.

The secondary motions associated with the "low" and "high" Dean-number regimes are found to be different. At low Dean numbers, the secondary motion is essentially the classical Dean-type circulation. At high Dean numbers, the occurrence of doubly peaked axial-velocity profiles appears also to coincide with the appearance of additional helical motions imbedded within the main Dean circulation. As the fully developed axial-velocity profiles are approached, these imbedded helical motions weaken and gradually disappear. Scarton et al. (1977) also report flow-visualization observations of additional inner-bend vortices in the entry-flow region, but their description of the motion is somewhat different from that of Agrawal et al. The existence of imbedded helical motions and of doubly peaked axial-velocity profiles has thus far not been predicted for pipes of circular cross section by theoretical or numerical analysis. However, doubly peaked profiles were found by Humphrey et al. (1977) in laminar flow at the exit of a 90° bend of square cross section under conditions of fully developed inlet conditions. Numerical calculations by these authors were in reasonable agreement with the measurements. Secondary velocities were not measured, but the calculated results suggest the presence of imbedded helical motions at the location where the axial profiles become double-peaked.

Although this review has dealt exclusively with laminar flows, it might be noted that measurements and calculations of turbulent flows in curved rectangular ducts exhibit many of the features observed in laminar flows. The interested reader is referred to Humphrey et al. (1981) and Taylor et al. (1982) for details and additional references.

Local wall-shear-rate measurements made by means of an electrochemical technique have been reported by Choi et al. (1979) and by Talbot & Wong (1982), for the same flow studied by Agrawal et al. Choi et al. found among other things that the wall regions adjacent to the locations of the imbedded helical secondary motions are regions of elevated shear

rate. The measurements of Talbot & Wong indicate that the point on the inner bend where the circumferential boundary layers first collide is a point of minimum shear rate, as predicted by Stewartson et al. (1980), but that the structure of the flow downstream of the collision point differs from that predicted.

The axial distance required for the attainment of the fully developed curved-pipe velocity profiles has been investigated by Austin (1971) for the case of a parabolic inlet profile. He reports his correlation in terms of the angular distance θ_D required, and gives $\theta_D = 49(\kappa\delta)^{1/3}$ (degrees). The data of Agrawal et al. suggest that Austin's result may underestimate slightly the development length for the case of a flat entry profile, but it is of the right order of magnitude.

The behavior of laminar pulsatile curved-pipe entry flow is of particular interest because of its relevance to flows in large blood vessels, as for example, the aortic arch, and has been investigated experimentally by Talbot & Gong (1982). Here in addition to the Dean number as a governing parameter, one has, as mentioned earlier, the frequency parameter $\bar{\alpha} = a(\omega/\nu)^{1/2}$ and the secondary-flow Reynolds number $R_s = \delta\hat{W}_a^2/\omega\nu$, which is a measure of the amplitude of the mean pulsatile axial-flow component $\hat{W}_a$. In the case of fully developed pulsatile flow in a curved pipe, Smith (1975) has identified at least ten different flow regimes, depending on the relative magnitudes of κ, $\bar{\alpha}$, and R_s. From the experiments of Talbot & Gong, it appears that Smith's classifications may in general be applicable to entry flow as well, at least insofar as indicating when the flow may be expected to be quasi-steady or when significant modifications of the secondary motions from their steady-flow values may be expected due to interaction with the pulsatile component of the axial flow. Hot-film-anemometer measurements by Chandran & Yearwood (1981), while not as extensive, are in general agreement with the measurements of Talbot & Gong.

Finally, we note that an interesting "resonance" between the axial and secondary flow has been reported by Lin & Tarbell (1980) for fully developed pulsatile flow. The resonance is found to occur when the period of pulsation is equal to the average time required for fluid to travel around the secondary-flow circuit, and is characterized by a sharp increase in the friction factor.

ACKNOWLEDGMENTS

The authors wish to express appreciation to Dr. George K. Lea, Program Director of the Fluid Mechanics Program of the National Science Foundation, for generous research support in this area under several NSF grants in his program. L.-S. Y. would also like to acknowledge partial support from Mr. M. K. Ellingsworth of the Office of Naval Research.

Literature Cited

Abul-Hamayel, M. A., Bell, K. J. 1979. Heat transfer in helically-coiled tubes with laminar flow. *ASME Pap. No. 79-WA/HT-11*

Adler, M. 1934. Strömung in gekrümmten Rohren. *Z. Angew. Math. Mech.* 14:257–75

Agrawal, Y., Talbot, L., Gong, K. 1978. Laser anemometer study of flow development in curved circular pipes. *J. Fluid Mech.* 85:497–518

Akiyama, M., Cheng, K. C. 1971. Boundary vorticity method for laminar forced convection heat transfer in curved pipes. *Int. J. Heat Mass Transfer* 14:1659–75

Akiyama, M., Cheng, K. C. 1974. Graetz problem in curved pipes with uniform wall heat flux. *Appl. Sci. Res.* 29:401–18

Austin, L. 1971. *The development of viscous flow within helical coils*. PhD thesis. Univ. Utah, Salt Lake City

Austin, L. R., Seader, J. D. 1973. Fully developed viscous flow in coiled circular pipes. *AIChE J.* 19:85–94

Barua, S. N. 1963. On secondary flow in stationary curved pipes. *Q. J. Mech. Appl. Math.* 16:61–77

Benjamin, T. B. 1978a. Bifurcation phenomena in steady flows of a viscous fluid. I. Theory. *Proc. R. Soc. London Ser. A.* 359:1–26

Benjamin, T. B. 1978b. Bifurcation phenomena in steady flows of a viscous fluid. II. Experiments. *Proc. R. Soc. London Ser. A.* 359:27–43

Berg, R. R., Bonilla, C. F. 1950. Heating of fluids in coils. *Trans. NY Acad. Sci.* 13:12–18

Blennerhassett, P. 1976. *Secondary motion and diffusion in unsteady flow in a curved pipe*. PhD thesis. Imperial Coll., London

Caro, C. G. 1966. The dispersion of indicator flowing through simplified models of the circulation and its relevance to velocity profile in blood vessels. *J. Physiol.* 185:501–19

Caro, C. G., Fitz-Gerald, J. M., Schroter, R. C. 1971. Atheroma and arterial wall shear: observation, correlation and proposal of a shear dependent mass transfer mechanism for atherogenesis. *Proc. R. Soc. London Ser. B* 177:109–59

Chandran, K. B., Yearwood, T. L. 1981. Experimental study of physiological pulsatile flow in a curved tube. *J. Fluid Mech.* 111:59–85

Chandran, K. B., Hosey, R. R., Ghista, D. N., Vayo, V. W. 1979. Analysis of fully developed unsteady viscous flow in a curved elastic tube model to provide fluid mechanical data for some circulatory path-physiological situations and assist devices. *J. Biomech. Eng.* 101: 114–23

Chandran, K. B., Swanson, W. M., Ghista, D. N. 1974. Oscillatory flow in thin-walled curved elastic tubes. *Ann. Biomed. Eng.* 2:392–412

Chandran, K. B., Yearwood, T. L., Wieting, D. M. 1979. An experimental study of pulsatile flow in a curved tube. *J. Biomech.* 12:793–805

Cheng, K. C., Akiyama, M. 1970. Laminar forced convection heat transfer in curved rectangular channels. *Int. J. Heat Mass Transfer* 13:471–90

Cheng, K. C., Lin, R-C., Ou, J-W. 1976. Fully developed laminar flow in curved rectangular channels. *J. Fluids Eng.* 98:41–48

Choi, U. S., Talbot, L., Cornet, I. 1979. Experimental study of wall shear rates in the entry region of a curved tube. *J. Fluid Mech.* 93:465–89

Coles, D. 1981. Prospects for useful research on coherent structure in turbulent shear flow. *Proc. Indian Acad. Sci. (Eng. Sci.)* 4:111–27

Collins, W. M., Dennis, S. C. R. 1975. The steady motion of a viscous fluid in a curved tube. *Q. J. Mech. Appl. Math.* 28:133–56

Collins, W. M., Dennis, S. C. R. 1976a. Steady flow in a curved tube of triangular cross-section. *Proc. R. Soc. London Ser. A* 352:189–211

Collins, W. M., Dennis, S. C. R. 1976b. Viscous eddies near a 90° and a 45° corner in flow through a curved tube of triangular cross-section. *J. Fluid Mech.* 76:417–32

Cuming, H. G. 1952. The secondary flow in curved pipes. *Aeronaut. Res. Counc. Rep. Mem. No. 2880*

Dean, W. R. 1927. Note on the motion of fluid in a curved pipe. *Philos. Mag.* 20:208–23

Dean, W. R. 1928. The streamline motion of fluid in a curved pipe. *Philos. Mag.* 30:673–93

Dean, W. R., Hurst, J. M. 1959. Note on the motion of fluid in a curved pipe. *Mathematika* 6:77–85

Dennis, S. C. R. 1980. Calculation of the steady flow through a curved tube using a new finite-difference method. *J. Fluid Mech.* 99:449–67

Dennis, S. C. R., Ng, M. 1980. Dual solutions for steady flow through a curved tube. *22nd Br. Theor. Mech. Colloq. Univ. Cambridge*

Dennis, S. C. R., Ng, M. 1982. Dual solutions for steady laminar flow through a curved tube. *Q. J. Mech. Appl. Math.* 35:305–24

Dravid, A. N., Smith, K. A., Merrill, E. W., Brian, P. L. T. 1971. Effect on secondary fluid motion of laminar flow heat transfer in helically coiled tubes. *AIChE J.* 17:1114–22

Erdogan, M. E. 1968. Laminar dispersion in a curved pipe. *Bull. Tech. Univ. Istanbul (Turkey)* 21:13–28

Erdogan, M. E., Chatwin, P. C. 1967. The effects of curvature and buoyancy on the laminar dispersion of solute in a horizontal tube. *J. Fluid Mech.* 29:465–84

Eustice, J. 1910. Flow of water in curved pipes. *Proc. R. Soc. London Ser. A* 84:107–18

Eustice, J. 1911. Experiments of streamline motion in curved pipes. *Proc. R. Soc. London Ser. A* 85:119–31

Fargie, D., Martin, B. W. 1971. Developing laminar flow in a pipe of circular cross-section. *Proc. R. Soc. London Ser. A* 321:461–76

Farthing, S. P. 1977. *Flow in the thoracic aorta and its relation to atherogenesis.* PhD thesis. Cambridge Univ.

Fry, D. L. 1968. Acute vascular endothelial changes associated with increased blood velocity gradients. *Circ. Res.* 22:165–97

Gould, T. L., Tek, M. R., Katz, D. L. 1974. Two-phase flow through vertical, inclined, or curved pipe. *J. Pet Technol.* 26:915–26

Greenspan, A. D. 1973. Secondary flow in a curved tube. *J. Fluid Mech.* 57:167–76

Grindley, J. H., Gibson, A. H. 1908. On the frictional resistance to the flow of air through a pipe. *Proc. R. Soc. London Ser. A* 80:114–39

Hasson, D. 1955. Streamline flow resistance in coils. *Res. Corresp.* 1:S1

Hausen, H. 1943. Darstellung des Warmeuberganges in Rohren durch verallgemeinerte Potenzbeziehungen. *Z. Ver. Dtsch. Ing., Beih. Verfahrenstech.* 4:91–98

Hawthorne, W. R. 1951. Secondary circulation in fluid flow. *Proc. R. Soc. London Ser. A* 206:374–87

Hayes, J. W., Hutton, J. F. 1972. Measurement of the normal stress coefficients of dilute polymer solutions from the flow in a curved tube. *Rheol. Acta* 11:89–92

Humphrey, J. A. C., Taylor, A. M. K., Whitelaw, J. H. 1977. Laminar flow in a square duct of strong curvature. *J. Fluid Mech.* 83:509–27

Humphrey, J. A. C., Whitelaw, J. H., Yee, G. 1981. Turbulent flow in a square duct with strong curvature. *J. Fluid Mech.* 103:443–63

Inaba, T., Murata, S. 1978. Pulsating laminar flow in a sinusoidally curved pipe. *Bull. JSME* 21:832–39

Itō, H. 1951. Theory on laminar flows through curved pipes of elliptic and rectangular cross-sections. *Rep. Inst. High Speed Mech., Tohoku Univ., Sendai, Jpn.*, Vol. 1, pp. 1–16

Itō, H. 1959. Friction factors for turbulent flow in curved pipes. *J. Basic Eng.* 81:123–34

Itō, H. 1960. Pressure losses in smooth pipe bends. *J. Basic Eng.* 82:131–43

Itō, H. 1969. Laminar flow in curved pipes. *Z. Angew. Math. Mech.* 49:653–63

Jain, R. K., Prabha, S. 1982. Gas-particulate flow through a curved pipe. *Z. Angew. Math. Mech.* 62:43–50

James, P. W. 1975. Unsteady elastico-viscous flow in a curved pipe. *Rheol. Acta* 14:679–87

Janssen, L. A. M., Hoogendoorn, C. J. 1978. Laminar convective heat transfer in helical coiled tubes. *Int. J. Heat Mass Transfer* 21:1179–1206

Jensen, M. K., Bergles, A. E. 1981. Critical heat flux in helically coiled tubes. *J. Heat Transfer* 103:661–66

Jensen, M. K., Bergles, A. E. 1982. Critical heat flux in helical coils with a circumferential heat flux tilt toward the outside surface. *Int. J. Heat Mass Transfer* 25:1383–95

Jones, D. T. 1967. *Some elastico-viscous flow problems.* PhD thesis. University Coll. of Wales, Aberystwyth

Jones, J. R. 1960. Flow of a non-Newtonian liquid in a curved pipe. *Q. J. Mech. Appl. Math.* 13:428–43

Joseph, B., Smith, E. P., Adler, R. J. 1975. Numerical treatment of laminar flow in helically coiled tubes of square cross-section. Part 1. Stationary helically coiled tubes. *AIChE J.* 21:965–74

Kaimal, M. R., Devanathan, R. 1980. Motion of a viscous fluid with suspended particles in a curved tube. *Int. J. Eng. Sci.* 18:847–54

Kalb, C. E., Seader, J. D. 1972. Heat and mass transfer phenomena for viscous flow

in curved circular tubes. *Int. J. Heat Mass Transfer* 15:801–17. Errata in *Int. J. Heat Mass Transfer* 15:2680

Kalb, C. E., Seader, J. D. 1974. Fully developed viscous-flow heat transfer in curved circular tubes with uniform wall temperature. *AIChE J.* 20:340–46

Kamel, M. T., Kaloni, P. N. 1977. On the flow of a Cosserat fluid through a curved pipe. *Z. Angew. Math. Phys.* 28:551–76

Kubair, V., Kuloor, N. R. 1966. Heat transfer to Newtonian fluids in coiled pipes in laminar flow. *Int. J. Heat Mass Transfer* 9:63–75

Larrain, J., Bonilla, C. F. 1970. Theoretical analysis of pressure drop in the laminar flow of fluid in a coiled pipe. *Trans. Soc. Rheol.* 14:135–47

Lighthill, M. J. 1970. Turbulence. In *Osborne Reynolds and Engineering Science Today*, ed. D. M. McDowell, J. D. Jackson, pp. 83–146. New York: Barnes & Noble

Lighthill, M. J. 1975. *Mathematical Biofluiddynamics*. Philadelphia: Soc. Ind. Appl. Math. 281 pp.

Lin, J. J., Tarbell, J. M. 1980. An experimental and numerical study of periodic flow in a curved tube. *J. Fluid Mech.* 100:623–38

Lin, T.-S. 1972. *Laminar convective transport processes in strongly curved tubes*. PhD thesis. Clarkson Coll. Technol., Potsdam, N.Y. 193 pp.

Liu, N.-S. 1976. Finite-difference solution of the Navier-Stokes equations for incompressible three-dimensional internal flows. *Proc. 5th Int. Conf. Numer. Methods Fluid Dyn.*, pp. 330–35

Liu, N.-S. 1977. Developing flow in a curved pipe. *INSERM-Euromech 92* 71:53–64

Lyne, W. H. 1971. Unsteady viscous flow in a curved pipe. *J. Fluid Mech.* 45:13–31

Maddock, C., Lacey, P. M. C., Patrick, M. A. 1974. *The structure of two-phase flow in a curved pipe*. Presented at Symp. Multi-Phase Flow Syst., Glasgow, April 2–4. Preprints in *Inst. Chem. Eng. Symp. Ser.* No. 38: Multi-Phase Flow Systems, March 1974

Manlapaz, R. L., Churchill, S. W. 1980. Fully developed laminar flow in a helically coiled tube of finite pitch. *Chem. Eng. Commun.* 7:57–78

Mashelkar, R. A., Devarajan, G. V. 1976a. Secondary flows of non-Newtonian fluids: Part I—Laminar boundary layer flow of a generalized non-Newtonian fluid in a coiled tube. *Trans. Inst. Chem. Eng.* 54:100–7

Mashelkar, R. A., Devarajan, G. V. 1976b. Secondary flow of non-Newtonian fluids: Part II. Frictional losses in laminar flow of purely viscous and viscoelastic fluids through coiled tubes. *Trans. Inst. Chem. Eng.* 54:108–14

Masliyah, J. H. 1980. On laminar flow in curved semicircular ducts. *J. Fluid Mech.* 99:469–79

McConalogue, D. J. 1970. The effects of secondary flow on the laminar dispersion of an injected substance in a curved tube. *Proc. R. Soc. London Ser. A* 315:99–113

McConalogue, D. J., Srivastava, R. S. 1968. Motion of fluid in a curved tube. *Proc. R. Soc. London Ser. A* 307:37–53

McDonald, D. A. 1974. *Blood Flow in Arteries*. Baltimore: Williams & Wilkins. 496 pp. 2nd ed.

Mishra, P., Gupta, S. N. 1979. Momentum transfer in curved pipes. I. Newtonian fluids. *Ind. Eng. Chem. Process Des. Dev.* 18:130–37

Morgan, G. W., Kiely, J. P. 1954. Wave propagation in a viscous liquid contained in a flexible tube. *J. Acoust. Soc. Am.* 26:323–28

Mori, Y., Nakayama, W. 1965. Study on forced convective heat transfer in curved pipes (1st Report, Laminar region). *Int. J. Heat Mass Transfer* 8:67–82

Mori, Y., Nakayama, W. 1967. Study on forced convective heat transfer in curved pipes (3rd Report). *Int. J. Heat Mass Transfer* 10:681–95

Mori, Y., Uchida, Y. 1967. Study on forced convective heat transfer in curved square channel. *Trans. Jpn. Soc. Mech. Eng.* 33:1836–46

Morimoto, T., Ousaka, A. 1974. A study of air-water two phase flow in a curved pipe. The effects of a 180° bend on the flow in upstream and downstream side straight pipes in the case of horizontal lines. *Sci. Pap. Fac. Eng. Tokushima Univ. (Japan) No. 19*, pp. 57–73

Mullin, T., Greated, C. A. 1980a. Oscillatory flow in curved pipes. Part 1. The developing flow case. *J. Fluid Mech.* 98:383–95

Mullin, T., Greated, C. A. 1980b. Oscillatory flow in curved pipes. Part 2. The fully developed case. *J. Fluid Mech.* 98:397–416

Munson, B. R. 1975. Experimental results for oscillating flow in a curved pipe. *Phys. Fluids* 18:1607–9

Murata, S., Miyake, Y., Inaba, T. 1976. Laminar flow in a curved pipe with varying curvature. *J. Fluid Mech.* 73:735–52

Murata, S., Miyake, Y., Inaba, T., Ogawa, H. 1981. Laminar flow in a helically coiled pipe. *Bull. JSME* 24:355–62

Nandakumar, K., Masliyah, J. H. 1982. Bifurcation in steady laminar flow through curved tubes. *J. Fluid Mech.* 119:475–90

Nerem, R. M., Cornhill, J. F. 1980. The role of fluid mechanics in atherogenesis. *J. Biomech. Eng.* 102:181–89

Nigam, K. D. P., Vasudeva, K. 1976. Influence of curvature and pulsations on laminar dispersion. *Chem. Eng. Sci.* 31:835–37

Nunge, R. J., Adams, L. R. 1973. Reverse osmosis in laminar flow through curved tubes. *Desalination* 13:17–36

Nunge, R. J., Lin, T.-S. 1973. Laminar flow in strongly curved tubes. *AIChE J.* 19:1280–81

Nunge, R. J., Lin, T.-S., Gill, W. N. 1972. Laminar dispersion in curved tubes and channels. *J. Fluid Mech.* 51:363–83

Oliver, D. R., Asghar, S. M. 1976. Heat transfer to Newtonian and viscoelastic liquids during laminar flow in helical coils. *Trans. Inst. Chem. Eng.* 54:218–24

Olson, D. E. 1971. *Fluid mechanics relevant to respiration — flow within curved or elliptical tubes and bifurcating systems.* PhD thesis. Imperial Coll., London

Owhadi, A., Bell, K. J., Crain, B. Jr. 1968. Forced convection boiling inside helically coiled tubes. *Int. J. Heat Mass Transfer* 11:1779–93

Patankar, S. V., Pratap, V. S., Spalding, D. B. 1974. Prediction of laminar flow and heat transfer in helically coiled pipes. *J. Fluid Mech.* 62:539–51

Patel, I. C., Sirs, J. A. 1977. Indicator dilution measurements of flow parameters in curved tubes and branching networks. *Phys. Med. Biol.* 22:714–30

Pedley, T. J. 1980. *The Fluid Mechanics of Large Blood Vessels*, Chap. 4, pp. 160–234. Cambridge Univ. Press.

Prusa, J., Yao, L.-S. 1982. Numerical solution of fully-developed flow in heated curved tubes. *J. Fluid Mech.* 123:503–22

Rabadi, N. J., Simon, H. A., Chow, J. C. F. 1980. Numerical solution for fully developed, laminar pulsating flow in curved tubes. *Numer. Heat Transfer* 3:225–39

Raju, K. K., Rathna, S. L. 1970. Heat transfer for the flow of a power-law fluid in a curved pipe. *J. Indian Inst. Sci.* 52:34–47

Richardson, P. D., Tanishita, K., Galletti, P. M. 1975. Mass transfer through tubes wound in serpentine shapes. *Lett. Heat Mass Transfer* 2:481–85

Riley, N., Dennis, S. C. R. 1976. *Flow in a curved pipe at high Dean numbers.* Presented at the Workshop on Viscous Interaction and Boundary-Layer Separation, Columbus, Ohio

Rushmore, W. L. 1975. *Theoretical investigation of curved pipe flows.* PhD thesis. State Univ. N.Y. at Buffalo. 160 pp.

Scarton, H. A., Shah, P. M., Tsapogas, M. J. 1977. Relationship of the spatial evolution of secondary flow in curved tubes to the aortic arch. In *Mechanics in Engineering*, pp. 111–31. Univ. Waterloo Press

Schilling, R., Simon, R. 1979. Berechnung der ausgebildeten Strömung in gekrümmten Kanälen mit rechteckigem Querschnitt. In *Recent Developments in Theoretical and Experimental Fluid Mechanics*, ed. U. Müller, K. G. Roesner, B. Schmidt. pp. 546–56. Berlin/Heidelberg: Springer-Verlag

Schlichting, H. 1979. *Boundary Layer Theory.* Transl. J. Kestin. New York: McGraw-Hill. 832 pp. 7th ed.

Schmidt, E. F. 1967. Wärmeübergang und Drukverlust in Rohrschlangen. *Chem. Ing. Tech.* 13:781–89

Seban, R. A., McLaughlin, E. F. 1963. Heat transfer in tube coils with laminar and turbulent flow. *Int. J. Heat Mass Transfer* 6:387–95

Sharma, H. G., Prakash, A. 1977. Flow of a second-order fluid in a curved pipe. *Indian J. Pure Appl. Math.* 8:546–57

Shaw, D. T., Rajendran, N. 1977. Diffusional deposition of airborne particles in curved bronchial airways. *J. Aerosol. Sci.* 8:191–97

Shchukin, V. K. 1969. Correlation of experimental data on heat transfer in curved pipes. *Therm. Eng.* 16:72–76

Simon, H. A., Chang, M. H., Chow, J. C. F. 1977. Heat transfer in curved tubes with pulsatile, fully developed, laminar flows. *J. Heat Transfer* 99:590–95

Singh, M. P. 1974. Entry flow in a curved pipe. *J. Fluid Mech.* 65:517–39

Singh, M. P., Sinha, P. C., Aggarwal, M. 1978. Flow in the entrance of the aorta. *J. Fluid Mech.* 87:97–120

Singh, R. P., Mishra, P. 1980. Friction factor for Newtonian and non-Newtonian fluid-flow in curved pipes. *J. Chem. Eng. Jpn.* 13:275–80

Singh, S. P. N., Bell, K. J. 1974. Laminar flow heat transfer in a helically-coiled

tube. *Proc. 5th Int. Heat Transfer Conf., Tokyo*, 2:193–97
Smith, F. T. 1975. Pulsatile flow in curved pipes. *J. Fluid Mech.* 71:15–42
Smith, F. T. 1976a. Steady motion within a curved pipe. *Proc. R. Soc. London Ser. A* 347:345–70
Smith, F. T. 1976b. Fluid flow into a curved pipe. *Proc. R. Soc. London Ser. A* 351:71–87
Smol'skiy, B. M., Chekhol'skiy, A. S. 1978. Investigation of heat and mass transfer in condensation of water vapor from moist air in curved channels. *Heat Transfer — Sov. Res. (USA)* 10(4):162–69
Squire, H. B., Winter, K. G. 1949. The secondary flow in a cascade of aerofoils in a non-uniform stream. *R.A.E. Rep. Aero 2317*
Srinivasan, S., Tien, C. 1971. Reverse osmosis in a curved tubular membrane duct. *Desalination* 9:127–39
Srivastava, R. S. 1980. On the motion of a fluid in a curved pipe of elliptical cross-section. *Z. Angew. Math. Phys.* 31:297–303
Srivastava, R. S., Sarin, V. B. 1973a. Heat transfer effects for an elastico-viscous fluid in a curved pipe. *Indian J. Pure Appl. Math.* 4:437–48
Srivastava, R. S., Sarin, V. B. 1973b. Heat transfer effects for an elastico-viscous fluid in a curved pipe of elliptic cross-section. *Indian J. Pure Appl. Math.* 4: 509–18
Stewartson, K., Simpson, C. J. 1982. On a singularity initiating a boundary-layer collision. *Q. J. Mech. Appl. Math.* 35:1–16
Stewartson, K., Cebeci, T., Chang, K. C. 1980. A boundary-layer collision in a curved duct. *Q. J. Mech. Appl. Math.* 33:59–75
Talbot, L., Gong, K. O. 1982. Pulsatile entrance flow in a curved pipe. *J. Fluid Mech.* In press
Talbot, L., Wong, S. J. 1982. A note on boundary layer collision in a curved pipe. *J. Fluid Mech.* 122:505–10
Tanishita, K., Nakano, K., Sakurai, Y., Hosokawa, T., Richardson, P. D., Galletti, P. M. 1978. Compact oxygenator design with curved tubes wound in weaving patterns. *Trans. Am. Soc. Artif. Intern. Organs.* 24:327–31
Tarbell, J. M., Samuels, M. R. 1973. Momentum and heat transfer in helical coils. *Chem. Eng. J.* 5:117–27
Taylor, A. K. M. P., Whitelaw, J. H., Yianneskis, M. 1982. Curved ducts with strong secondary motion: velocity measurements of developing laminar and turbulent flow. *J. Fluids Eng.* In press
Taylor, G. I. 1929. The criterion for turbulence in curved pipes. *Proc. R. Soc. London Ser. A* 124:243–49
Texon, M. 1960. The hemodynamic concept of atherosclerosis. *Bull. NY Acad. Med.* 36:263–74
Thomas, R. H., Walters, K. 1963. On the flow of an elastico-viscous liquid in a curved pipe under a pressure gradient. *J. Fluid Mech.* 16:228–42
Thomas, R. H., Walters, K. 1965. On the flow of an elastico-viscous fluid in a curved pipe of elliptic cross-section under a pressure gradient. *J. Fluid Mech.* 21:173–82
Thomson, J. 1876. On the origin of windings of rivers in alluvial plains, with remarks on the flow of water round bends in pipes. *Proc. R. Soc. London Ser. A* 25:5–8
Thomson, J. 1877. Experimental demonstration in respect to the origin of windings of rivers in alluvial plains, and to the mode of flow of water round bends of pipes. *Proc. R. Soc. London Ser. A.* 26:356–57
Topakoglu, H. C. 1967. Steady laminar flows of an incompressible viscous fluid in curved pipes. *J. Math. Mech.* 16:1321–38
Truesdell, L. C., Adler, R. J. 1970. Numerical treatment of fully developed laminar flow in helically coiled tubes. *AIChE J.* 16:1010–15
Tsang, H. Y., James, D. F. 1980. Reduction of secondary motion in curved tubes by polymer additives. *J. Rheol.* 24:955–56
Van Dyke, M. 1978. Extended Stokes series: laminar flow through a loosely coiled pipe. *J. Fluid Mech.* 86:129–45
Wang, C. Y. 1981. On the low-Reynolds-number flow in a helical pipe. *J. Fluid Mech.* 108:185–94
Ward-Smith, A. J. 1968. *Some aspects of fluid flow in ducts.* D. Phil. thesis. Univ. Oxford
Ward-Smith, A. J. 1980. *Internal Fluid Flow*, pp. 278–98. Oxford Univ. Press
Weissman, M. H., Mockros, L. F. 1968. Gas transfer to blood flowing in coiled circular tubes. *ASCE Proc., Eng. Mech. Div. J.* 94:857–72
Whalley, P. B. 1980. Air-water two-phase flow in a helically coiled tube. *Int. J. Multiphase Flow* 6:345–56

White, C. M. 1929. Streamline flow through curved pipes. *Proc. R. Soc. London Ser. A* 123:645–63

Williams, G. S., Hubbell, C. W., Fenkell, G. H. 1902. Experiments at Detroit, Mich., on the effect of curvature upon the flow of water in pipes. *Trans. ASCE* 47:1–196

Womersley, J. R. 1957. The mathematical analysis of the arterial circulation in a state of oscillatory motion. *Tech. Rep. WADC-TR 56-614*, Wright Air Dev. Cent.

Yalamov, Y. I., Muradyan, S. M. 1980. Trajectories and capture coefficient of aerosol-particles in curved channels. *Zh. Tekh. Fiz.* 50:400–2

Yao, L.-S., Berger, S. A. 1975. Entry flow in a curved pipe. *J. Fluid Mech.* 67:177–96

Yao, L.-S., Berger, S. A. 1978. Flow in heated curved pipes. *J. Fluid Mech.* 88:339–54

Yeung, W.-S. 1979. Erosion in a curved pipe. *Wear* 55:91–106

Yeung, W.-S. 1980. Laminar boundary-layer flow near the entry of a curved circular pipe. *J. Appl. Mech.* 47:697–702

Zalosh, R. G., Nelson, W. G. 1973. Pulsating flow in a curved tube. *J. Fluid Mech.* 59:693–705

Zapryanov, Z., Christov, Ch. 1977. Fully developed flow of viscous incompressible fluid in toroidal tube with circular cross-section. *Theor. Appl. Mech.* 8:11–17

Zapryanov, Z., Matakiev, V. 1980. An exact solution of the problem of unsteady fully-developed viscous flow in slightly curved porous tube. *Arch. Mech. (Poland)* 32:461–74

Zapryanov, Z., Christov, C., Toshev, E. 1980. Fully developed laminar flow and heat transfer in curved tubes. *Int. J. Heat Mass Transfer* 23:873–80